NRL Report 8056

A Spectral Atlas of the Sun Between 1175 and 2100 Angstroms

O. KJELDSETH MOE, M. E. VANHOOSIER,
J.-D. F. BARTOE, AND G. E. BRUECKNER

E. O. Hulburt Center for Space Research

December 31, 1976

NAVAL RESEARCH LABORATORY
Washington, D.C.

SECURITY CLASSIFICATION OF THIS PAGE (*When Data Entered*)

REPORT DOCUMENTATION PAGE		READ INSTRUCTIONS BEFORE COMPLETING FORM
1. REPORT NUMBER NRL Report 8056	2. GOVT ACCESSION NO.	3. RECIPIENT'S CATALOG NUMBER
4. TITLE (*and Subtitle*) A SPECTRAL ATLAS OF THE SUN BETWEEN 1175 and 2100 ANGSTROMS		5. TYPE OF REPORT & PERIOD COVERED Final report on one phase of a continuing NRL Problem.
		6. PERFORMING ORG. REPORT NUMBER
7. AUTHOR(s) O. Kjeldseth Moe, M.E. VanHoosier, J.-D. F. Bartoe, and G.E. Brueckner		8. CONTRACT OR GRANT NUMBER(s)
9. PERFORMING ORGANIZATION NAME AND ADDRESS Naval Research Laboratory Washington, D.C. 20375		10. PROGRAM ELEMENT, PROJECT, TASK AREA & WORK UNIT NUMBERS 71A01-24A
11. CONTROLLING OFFICE NAME AND ADDRESS National Aeronautical and Space Administration Washington, D.C. 20546		12. REPORT DATE December 31, 1976
		13. NUMBER OF PAGES 61
14. MONITORING AGENCY NAME & ADDRESS(*if different from Controlling Office*)		15. SECURITY CLASS. (*of this report*) Unclassified
		15a. DECLASSIFICATION/DOWNGRADING SCHEDULE

16. DISTRIBUTION STATEMENT (*of this Report*)

Approved for public release; distribution unlimited.

17. DISTRIBUTION STATEMENT (*of the abstract entered in Block 20, if different from Report*)

18. SUPPLEMENTARY NOTES

19. KEY WORDS (*Continue on reverse side if necessary and identify by block number*)

Aeronomy
Quasar UV spectra
Stellar UV spectra
Solar UV intensity
Solar UV spectra
Solar UV continuum

20. ABSTRACT (*Continue on reverse side if necessary and identify by block number*)

This atlas provides solar spectra with high spectral resolution which will satisfy the needs of both solar physics and aeronomy for information on the solar spectrum in the wavelength range 1175 to 2100 Angstroms. The spectra may furthermore be useful for comparison with stellar UV spectra and with the red shifted spectra of quasars. Specific intensities as functions of wavelength are shown for two quiet regions between 1175 and 2100 Angstroms and for one active region between 1680 and 2100 Angstroms. The two quiet regions, located at heliocentric

(Continued)

DD FORM 1 JAN 73 1473 EDITION OF 1 NOV 65 IS OBSOLETE
S/N 0102-014-6601

 SECURITY CLASSIFICATION OF THIS PAGE (*When Data Entered*)

20. Abstract (Continued)

positions cos θ = 0.73 and cos θ = 0.32, represent a disk and a limb spectrum of the sun. The absolute intensities are determined with an accuracy of ±25% and the wavelength scale is accurate to 0.025 Angstroms. The spectral resolution is 0.07 Angstroms.

CONTENTS

A SPECTRAL ATLAS OF THE SUN BETWEEN 1175 AND 2100 ANGSTROMS

1. INTRODUCTION

Atlases of the solar ultraviolet radiation have been presented for the wavelength region 2226 - 2992 Å by Tousey et al. [1] and for the region 2988 - 3629 Å by Brueckner [2]. However, correspondingly complete information on line profiles and continua with good spectral resolution and reliable calibration of absolute intensity have not been published for wavelengths below 2226 Å. This atlas will satisfy in part the needs of both solar physics and aeronomy for information on the solar spectrum in this wavelength region.

Because the solar spectrum, particularly the emission lines, varies considerably in intensity between the quiet disk and limb and between quiet and active regions, we have included spectra from all three types of regions, wherever material was available.

In order to provide an atlas which allows greater reading accuracy, a limited quantity of 12 by 21 inch hardbound copies are available as NRL Report 8057. The spectra are also available on magnetic computer tapes (see Appendix A). Furthermore, a publication is being prepared listing the intensities averaged over wavelength intervals ranging from 0.1 to 10.0 Å bandwidths.

The reliability of the intensities presented in the atlas can be judged by comparison with results obtained by other observers. Extensive comparisons of this kind have been made by Brueckner et al. [3], Kjeldseth Moe et al. [4], and VanHoosier et al. [5]. Absolute intensities derived from the atlas and converted into solar mean intensity or intensity at the center of the disk are shown to be in good agreement with recent measurements by Rottman [6], Heroux and Swirbalus [7], Simon [8], Samain et al. [9], and Samain and Simon [10]. In making these comparisons we took great care to deresolve our high-resolution spectra to fit the lower resolution used by these authors. The agreement is illustrated in Fig. 1, showing the mean intensity of the sun averaged over 10 Å intervals as given by various observers. For this figure the atlas intensities at 300″ inside the limb were converted to solar mean intensities using the center-to-limb variations given by Samain et al. [9]. All the intensities agree within our error limit of ±25%.

In the following, Sec. 2 explains how to read the atlas graphs, and Sec. 3 to 6 describe the observations, the photometry and data handling, the wavelength scale, and the absolute intensity calibration.

2. DESCRIPTION OF THE ATLAS

The atlas presents the absolute intensity of two quiet regions between 1175 Å and 2100 Å. One region is located 300″ inside the solar limb ($\cos \theta = 0.73$) and is representative of the spectrum of most of the disk. The other quiet region is located 50″ inside

Manuscript submitted August 27, 1976.

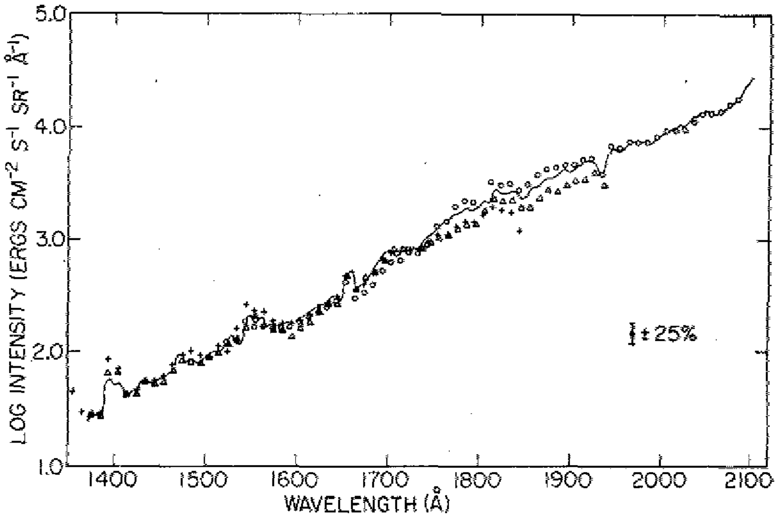

Fig. 1 — Comparison of solar mean intensities averaged over 10 Å intervals. The full line represent the NRL CALROC data used in the atlas. Open circles are the observations of Samain and Simon [10], crosses the observations of Rottman [6], and triangles the observations of Heroux and Swirbalus [7].

the limb (cos θ = 0.32) and is more representative of a limb spectrum. In addition, the spectrum of an active region is presented for wavelengths greater than 1680 Å.

The atlas gives the logarithm of the specific intensity in erg cm^{-2} s^{-1} sr^{-1} $Å^{-1}$ vs wavelength in Angstroms. The spectra of the quiet regions and the active region are plotted above each other on the same page. This facilitates comparison of details in the three types of spectra. The tracings of the different regions are distinguished by the labels 300", 50", and AR on the right-hand side of each page.

On the wavelength axis every 0.1 Å has been marked off, with heavier marks for every full Angstrom. The scale along the intensity axis is determined by the distance between neighboring tick marks, corresponding to logarithmic intensity intervals $\Delta \log_{10}$ (intensity) = 0.10. For clarity the spectra of the different pointings are plotted displaced from each other. Reference values for the displaced logarithmic intensity scales are given by the annotations on the intensity axis on the left-hand side of each page. The annotations are placed roughly on a level with their corresponding intensity tracing, and annotated tick marks are drawn somewhat longer than the others. The numbers give the logarithm of the intensity at the annotated tick mark.

For wavelengths below 1400 Å only isolated emission lines are displayed. The continuum between lines is here too weak to be recorded even with the longest exposure times (see Table 1). For wavelengths below 1200 Å only the emission lines at the limb position (50") are shown; the corresponding spectral features on the disk (300") fall below the detection limit. The active region spectrum is shown only at wavelengths above 1680 Å because exposure conditions during flight did not permit reliable calibration for shorter wavelengths.

Table 1 — Data for Exposures Used to Make the Atlas

Date	Target	Exposure Time (s)	Altitude at Start of Exposure (km)
Sept. 4, 1973	Active Region	5.45	120.4
	McMath 508	1.07	111.3
Jan. 15, 1974	300″ ± 30″	55.45	174.0
		1.95	218.7
		9.45	220.1
		31.45	224.8
	50″	39.45	234.2
		3.45	230.6
		9.45	227.4
		111.45	225.9

3. OBSERVATIONS

The spectra used for preparing the atlas were taken during the calibration rocket (CALROC) flights made on Sept. 4, 1973, and Jan. 15, 1974. The purpose of the CALROC flights was to calibrate the Naval Research Laboratory spectrographs on the Apollo Telescope Mount on Skylab. The telescope of the CALROC instrument is an off-axis parabola of 1-m focal length, focusing a solar image onto a spectrograph slit. The slit covers an area of 2″ by 60″ on the solar disk; this defines the spatial resolution of the instrument. There is no resolution along the slit. The spectrograph photographs the spectrum from 1175 to 2100 Å in the first order of the main grating, with a spectral resolution of 0.07 Å and a linear dispersion of 4.75 Å/mm. A more detailed description of the instrument is given by Brueckner et al. [3]. The spectra were photographed on Eastman Kodak 104 film, which is less susceptible to hypersensitization than the more sensitive 101 emulsion. On the 1973 flight, observations were made with the slit parallel to the limb and pointing at four quiet sun positions, at distances 300″, 50″, 25″ and 12″ inside the limb. In addition spectra were taken in active region McMath 508. The active region spectrum in the atlas is derived from these exposures.

The 1973 flight probably had the most reliable intensity calibration (see Sec. 6). However, the pointing of the instrument during the longest exposure at 300″ was not stable.

During this exposure the slit pointed first outside the limb and then at positions between the limb and 300″ before coming to rest at the latter position. As a result, for this pointing only the stronger emission lines were registered at wavelengths below 1700 Å.

For the calibration flight of Jan. 15, 1974, it was decided to point at only two positions on the quiet sun: 300″ and 50″ inside the limb. Long exposure times were used to record as much of the weak continuum below 1700 Å as possible. For this reason the quiet sun spectra in the atlas are based mainly on the exposures of this flight.

Information on the exposures used to prepare the atlas is given in Table 1. For the exposures at 50″ inside the limb and in the active region, the full spatial resolution of the instrument (2″ by 60″) was used. During the exposures at 300″ inside the limb the slit was moved back and forth perpendicular to its length, covering an area of about 60″ by 60″ on the solar disk. This was done to average the inhomogeneous solar emission associated with the chromospheric network.

The quiet solar regions were selected carefully to avoid any solar activity, coronal holes, or filament channels. For this we used Hα and K-line filtergrams and the coronal images transmitted daily from the NRL XUV monitor on Skylab [11]. In the case of the active region 90% of the slit was covered by the plage. Figure 2 is a detailed drawing of the location of the spectrograph slit inside the plage.

4. DATA REDUCTION

The CALROC flight spectra appear on the film as narrow strips 200 mm long and 300 μm wide. Because of an uneven intensity distribution in the direction perpendicular to the dispersion, only the central 120-μm-wide part of the spectrum has been used for photometry. The spectrum is curved along the direction of dispersion, the ends of the spectrum deviating several hundred micrometers from the tangent of the middle portion.

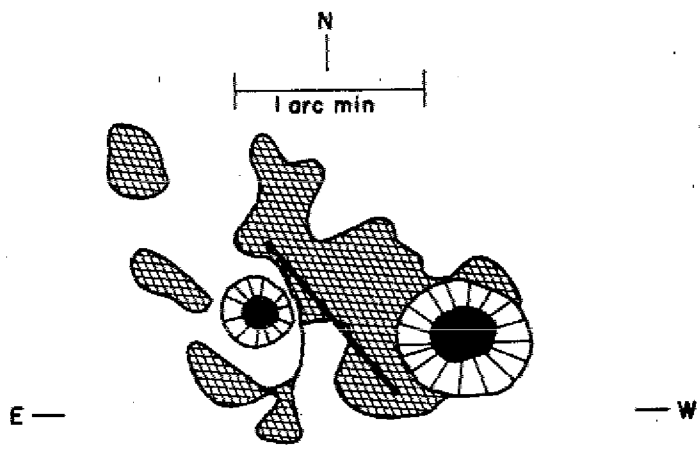

Fig. 2 — Position of the spectrograph slit inside active region McMath 508 on September 4, 1973.

Consequently the photometry was performed in short segments of 5 mm (22 Å) length. This ensured that the entire photometer slit always stayed in the region of uniform exposure.

The film characteristic curve had to be constructed from the flight exposures. The method consisted of comparing film densities above fog level at exactly the same wavelengths on exposures taken with different exposure times but at the same pointing. For each wavelength point this produced a set of values of film densities and corresponding logarithms of exposure times. The sets for the various wavelengths were then shifted independently along the exposure axis until a best fit to an average curve was obtained. An example of such a curve is given in Fig. 3. This particular curve was made up from a narrow region ($\Delta\lambda \approx 0.2$ Å) around 1745 Å. This method assumes that a possible reciprocity failure is small and can be disregarded.

Representative spectral regions were selected throughout the wavelength range. We found the shape of the relative characteristic curve to be independent of wavelength within the error limits. An average curve could thus be applied to all of the film exposed during each flight. However, the curves for the two flights were slightly different.

Only a small fraction of the spectra (less than 1%) was used to derive the relative characteristic curves. However, the curves were found to apply to the rest of the data with equally good accuracy. The scatter of the observed points around the average curves corresponded to an error in the relative intensities of approximately ±10% for the quasi-linear part of the curves.

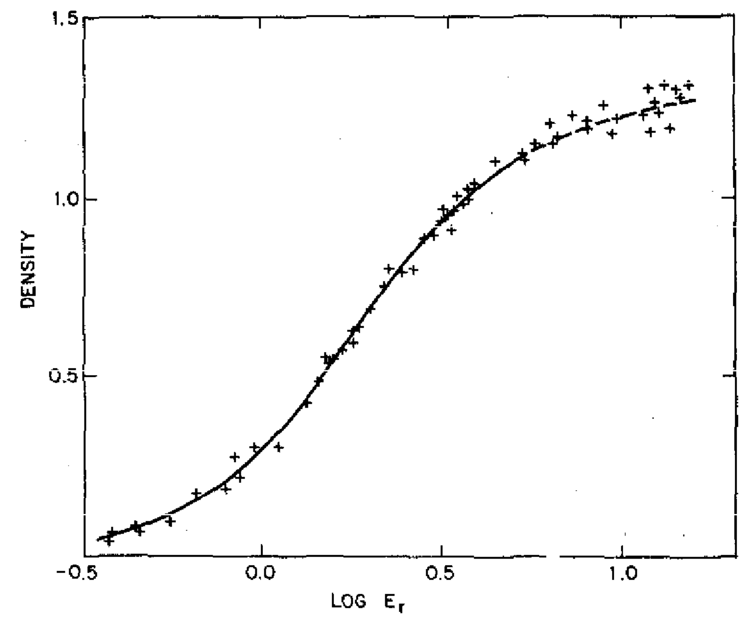

Fig. 3 — Example of film characteristic curve determined from the flight exposures. Crosses mark the observed points shifted along the exposure axis to form the best possible average curve.

In the toe and particularly in the shoulder of the film characteristic curve the relative photometry is less accurate than ±10%. The most reliable part of the curve was taken to be between densities of 0.07 and 0.75 above fog. Photometry generally was not performed for film densities outside these limits. Exceptions are the weak continuum at short wavelengths ($\lambda \approx 1400$ Å), extending below the low density limit even for the longest exposure times, and a small number of very strong emission lines where the photometry of the line peaks had to be extended into the shoulder region.

From Fig. 3 the entire range in exposure available from the reliable portion of the characteristic curve for a single exposure is seen to be 0.9 in logarithmic units. However, the solar continuum from 1400 to 2100 Å covers an intensity range of almost four orders of magnitude. Furthermore, even in narrow spectral intervals containing strong lines, the densities of a single exposure frequently vary beyond the range of the reliable portion of the characteristic curve. Thus, in almost all wavelength regions the atlas had to be fitted together from exposures made with several different exposure times. In matching two exposures of the same spectral region the corresponding points in both exposures were required to lie on the most reliable part of the film characteristic curve. This means that the shape of strong emission line profiles can be regarded as accurate over the entire profile.

The Lyα line presented a special problem. On the 1974 CALROC flight this line became seriously overexposed in the line core, even for the shortest exposure times at the 50″ and 300″ pointings. The central region (1 Å wide) of the line was therefore omitted from the atlas.

The intensity scans presented in the atlas have been smoothed by removing high-frequency noise in the film emulsion and photometry using a Fourier filtering technique described by Nicolas et al. [12]. A low-frequency component caused by grain clumps in the emulsion of size 10 μm could not be removed by filtering without degrading the effective instrumental width. These grain clumps may distort slightly the intensities and profiles.

The broadening caused by the instrument profile has not been removed from the atlas spectra, because the shape of the instrument profile is not known in enough detail. Furthermore, the low-frequency noise component still present in the data may cause strong distortions if deconvolution is attempted. One may estimate the line widths from

$$\Delta\lambda_T \approx (\Delta\lambda_o^2 - \Delta\lambda_I^2)^{1/2}$$

where $\Delta\lambda_o$ is the observed line width, $\Delta\lambda_I$ the instrumental width, and $\Delta\lambda_T$ the true width of the line profile. Theoretical calculations using a ray-tracing method gave a constant instrumental width of 0.055 Å for all wavelengths between 1200 and 2100 Å. This should be regarded as a lower limit since the effect of the film emulsion has not been taken into account. From the width of the narrowest emission lines in the spectrum, it seems more likely that the effective instrumental width is 0.07 Å.

5. THE WAVELENGTH SCALE

The wavelength scale of the atlas was established by carefully measuring the positions of selected standard lines with well-known laboratory wavelengths, which were unblended and symmetric in the solar spectrum. If one measured the photographically recorded flight spectrum using a comparator it would be possible to determine wavelengths accurate to 0.005 Å over a range of 300-400 Å. For the atlas it was not possible to establish the wavelengths this accurately. Owing to the rather short wavelength sections included by each scan and the realignment of the photometer table necessary to adjust for the curvature of the spectrum, each section contained only a few suitable standard lines.

We tried to base the wavelength scale on a uniform selection of standard lines. The Si I and C I lines are considered the most reliable standards in this part of the spectrum. The laboratory wavelengths for these lines were taken from Moore [13,14]. However, Si I and C I lines were not present in all wavelength sections, and we had to rely mainly on Fe II emission lines between 1650 Å and 1750 Å, on Fe I absorption lines at wavelengths above 1950 Å, and on S I lines scattered throughout the spectral range. For lines below 2000 Å, other than the Si I and C I lines, laboratory wavelengths were taken from Kelly and Palumbo [15]. Above 2000 Å the wavelengths listed by Moore [16] were used.

It was possible to fit a wavelength scale to the selected standard lines with an accuracy of ±0.025 Å over most of the wavelength region covered by the atlas. The only exceptions were a few of the short wavelength sections where the wavelength scale had to be determined from lines of multiply-ionized atoms because these were the only lines strong enough to be recorded.

6. INTENSITY CALIBRATION

The intensities given in this atlas are based on calibrations made especially for the rocket instrument. They do not rely on comparison with any previous solar observations made with a different instrument. In this section we give only a brief summary of the instrument calibration, with emphasis on a few points of special interest in connection with the observation material used for the atlas. For a detailed description of the calibration procedures and the errors involved we refer to papers by Brueckner et al. [3] for $\lambda > 1750$ Å and Kjeldseth Moe et al. [4] for 1250 Å $< \lambda < 1750$ Å.

In the wavelength region 1750-2100 Å, the calibration was made using a deuterium lamp as a secondary standard. The deuterium lamp, having a continuous spectrum above 1680 Å, was calibrated by the National Bureau of Standards (NBS) against a hydrogen arc which served as the primary standard [17,18].

Segments of the D_2 continuum were photographed, prior to flight, on each strip of flight film just below the flight exposure. Short of in-flight calibration, this method is the best possible for reducing errors resulting from film inhomogeneities, development effects, and film environment effects during flight. In addition, series of deuterium lamp spectra were taken before and after flight on separate strips of film, to detect any changes in instrument sensitivity.

Shortward of 1680 Å the deuterium lamp could not be used as a calibration standard because of the appearance of numerous D_2 molecular emission lines. In this wavelength region the rocket instrument was calibrated after flight, using a recently developed argon arc as the standard. The intensity of the argon arc was determined as a function of wavelength between 1250 Å and 3000 Å at NBS [19].

We used the argon arc merely as a standard of relative spectral intensity to determine the variation of the rocket instrument sensitivity with wavelength. The sensitivity of instrument and film for wavelengths below 1750 Å was placed on an absolute scale by adjusting this relative calibration to the absolute calibration above 1750 Å from the deuterium lamp exposures on the flight film.

Thus it was assumed that the wavelength dependence of the sensitivity of instrument and film was unchanged between the time of the CALROC flights and that of the argon arc calibration. This assumption is supported by the agreement in shape between the spectral sensitivity curves determined from the original flight calibration for $\lambda > 1700$ Å and similar sensitivity curves obtained at the time of the argon arc calibration.

Shortward of 1250 Å the sensitivity has been extrapolated. This becomes increasingly unreliable below 1200 Å, where the instrument reflectivity begins to fall off rather sharply.

For the 1973 CALROC flight the preflight and postflight sensitivities from the deuterium lamp agreed to better than 10%. It was possible from these exposures to determine the film characteristic curve with an absolute exposure scale as a function of wavelength. The applicability of this characteristic curve to the flight film was confirmed by measuring the intensity of the deuterium lamp segments placed on the flight film and comparing with the intensity values given by the lamp calibration.

For the atlas exposures from the 1974 flight, the instrument could not be calibrated from the preflight and postflight sensitivity checks. The preflight deuterium lamp exposures were not developed together with the flight film. Furthermore, the postflight exposures had a defect in the emulsion that destroyed the quasi-linear relationship between film density and log exposure at densities larger than 0.45 above fog. Thus no reliable check of possible sensitivity changes of the spectrograph could be made. For this reason we believe the intensities obtained on the 1973 CALROC flight to be the most reliable. A comparison in the intensities at 300″ determined on the two flights showed that the slopes of the spectra with wavelength were identical between 1750 Å and 2100 Å. However, the intensities of the 1973 flight were systematically 27% lower than those of the 1974 flight. While this difference is fairly large, the results are still in agreement within the estimated rms errors of ±20% for the 1973 flight and ±25% for the 1974 flight [3,4].

It was decided to adjust the intensities of the quiet regions in the atlas to an average level between the values determined for the 1973 and 1974 flights. We estimate the given absolute intensities to be accurate to within ±25%. The accuracy of relative photometry, such as the shape of a line profile, is of course much better (see Sec. 4).

ACKNOWLEDGMENT

The material used for this atlas was part of NRL's ATM observations, and we would like to thank the Principal Investigator, Dr. R. Tousey, for his support.

This work was also supported by NASA DPR-S-60404-G.

REFERENCES

1. R. Tousey, E. F. Milone, J. D. Purcell, W. Palm Schneider, and S. G. Tilford, "An Atlas of the Solar Ultraviolet Spectrum Between 2226 and 2992 Angstroms," NRL Report 7788, 1974.

2. G. Brueckner, *Photometric Atlas of the Near Ultraviolet Solar Spectrum 2988 Å-3629* Å, Vandenhoeck and Ruprecht, Göttingen, 1960.

3. G. E. Brueckner, J.-D. F. Bartoe, O. Kjeldseth Moe, and M. E. VanHoosier, *Ap. J.*, 209, 935, 1976.

4. O. Kjeldseth Moe, J.-D. F. Bartoe, G. E. Brueckner, and M. E. VanHoosier, to be published in *Ap. J.* (1977).

5. M. E. VanHoosier, J.-D. F. Bartoe, G. E. Brueckner, and O. Kjeldseth Moe, to be published in *J. Geophys. Res.* (1977).

6. G. J. Rottman, *Trans. Amer. Geophys. Union* 56, 1157 (1974).

7. L. Heroux and R. A. Swirbalus, *J. Geophys. Res.* 81, 436 (1976).

8. P. C. Simon, in *Proceedings of the Third Conference on the Climatic Impact Assessment Program*, p. 137, A. J. Broderick and T. M. Hard, eds., DOT-TSC-OST-74-15, 1974.

9. D. Samain, R. M. Bonnet, R. Gayet, and C. Lizambert, *Astron. Astrophys.* 39, 71 (1975).

10. D. Samain and P. C. Simon, to be published in *Solar Physics*, 1977.

11. W. R. Crockett, N. P. Patterson, J. D. Purcell, R. J. Schumacher, and R. Tousey, to be published in *Appl. Opt.* (1977).

12. K. R. Nicolas, G. E. Brueckner, R. Tousey, D. A. Tripp, O. E. White, and R. G. Athay, submitted to *Solar Physics* (1977).

13. C. E. Moore, *Selected Tables of Atomic Spectra*, Sec. 2, NSRDS-NBS 3, 1967.

14. C. E. Moore, *Selected Tables of Atomic Spectra*, Sec. 3, NSRDS-NBS 3, 1970.

15. R. L. Kelly and L. J. Palumbo, "Atomic and Ionic Emission Lines Below 2000 Angstroms," NRL Report 7599, 1973.

16. C. E. Moore, "An Ultraviolet Multiplet Table," Secs. 1 and 2, National Bureau of Standards Circular 488, 1950.

17. W. R. Ott, P. Fieffe-Prevost, and W. L. Wiese, *Appl. Opt.* 12, 1618 (1973).

18. W. R. Ott, K. Behringer, and G. Gieres, *Appl. Opt.* 14, 2121 (1975).

19. J. M. Bridges and W. Ott, to be published in *Appl. Opt.* (1977).

Note added in proof:

A recent reflight of the calibration rocket instrument has yielded intensities of the emission lines shortward of 1400 Å that are significantly higher than the intensities in the atlas (p. 12 to 23). At reflight the instrument was calibrated both before and after flight using the argon arc, thus differing from the CALROC flights where the argon arc calibration was performed 6 months after the last flight. (The argon arc was not developed until this time).

The difference in calibration below 1400 Å between the reflown instrument and the CALROC was probably caused by an undetected contamination of the collimator mirror used during calibration of the CALROC instrument. Such contamination would have occurred between June 3, 73 when the mirror was used during the calibration exposures and July 11, 73 when its reflectivity was measured.

Figure 4 shows the logarithm of the ratio of intensities observed with the reflown instrument and the atlas intensities as a function of wavelength. Only lines from neutral and singly ionized atoms were compared since the intensities of multiply ionized atoms change too much across the surface of the sun to be reliably compared. The broken line represents the best average curve through the data. We believe the atlas intensities between 1250 Å and 1400 Å should be corrected upward using the data given in Figure 4. At wavelengths below 1250 Å there are no lines visible that are suitable for a reliable comparison. Evidence from multiply ionized lines suggests a correction factor of 1.5 to 3.0. The reflown instrument measures an irradiance of 4.8 erg cm^{-2} s^{-1} for Lyα, which is in good agreement with most recent observations.

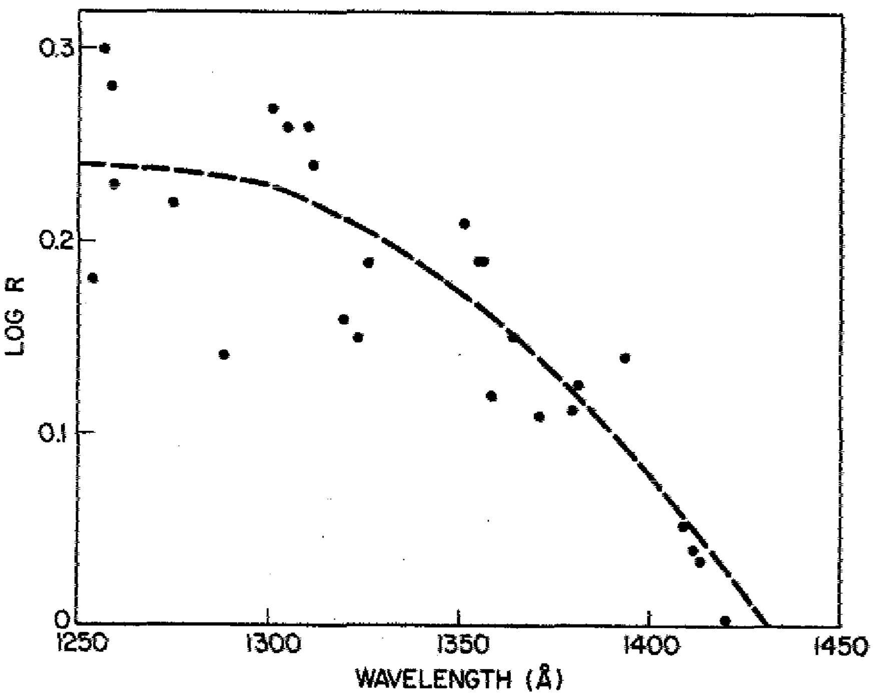

Fig. 4 — Ratio of intensities, reflown instrument, to CALROC.

Appendix A
COMPUTER TAPE FORMAT

Magnetic computer tapes containing the Atlas information are available from the World Data Center-A for Rockets and Satellites located at the National Space Science Data Center (NSSDC) NASA, Greenbelt, Maryland 20771 (USA) under the identification number RS-12A. There are 47 files on each tape, one file for each Atlas page, and 3 records in each file. The first record contains the 300″ data, the second record is for the 50″, and the third is from the active region. The records are 4201 words long with the first word equal to the starting wavelength of the record and with 4200 words containing the 21Å of logarithmic intensity at intervals of 0.005Å. Values of zero indicate that data was not available at that wavelength. The data are 48-bit floating-point words (CDC 3800 computer binary format) written at 556 BPI, odd parity on 7 track tape. NSSDC can supply tapes in a format suitable for virtually any standard computer to facilitate the processing by the requesting user. NSSDC should be contacted directly concerning the format and ordering information.

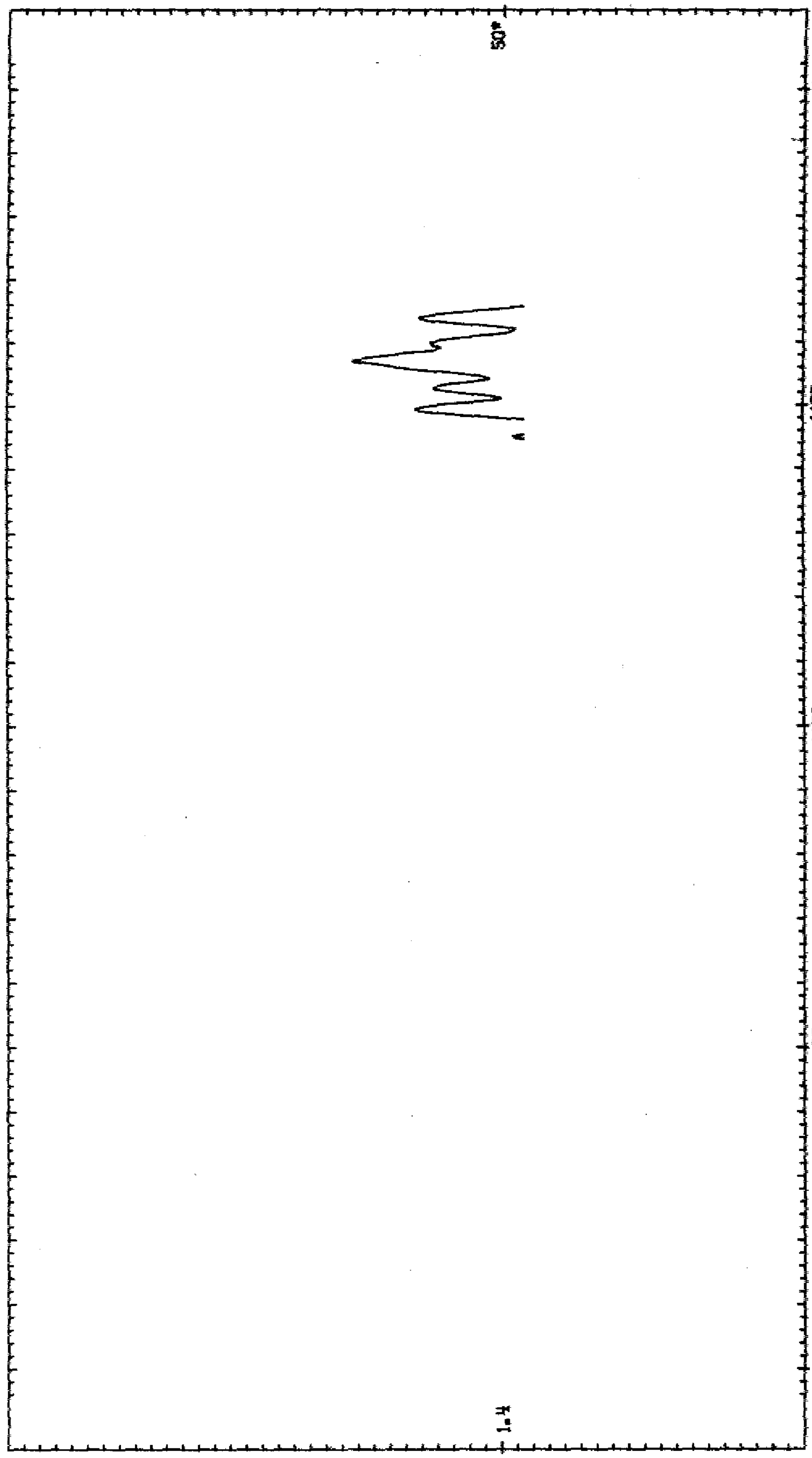
50*
1.4
1160
1165
1170
1175
1180

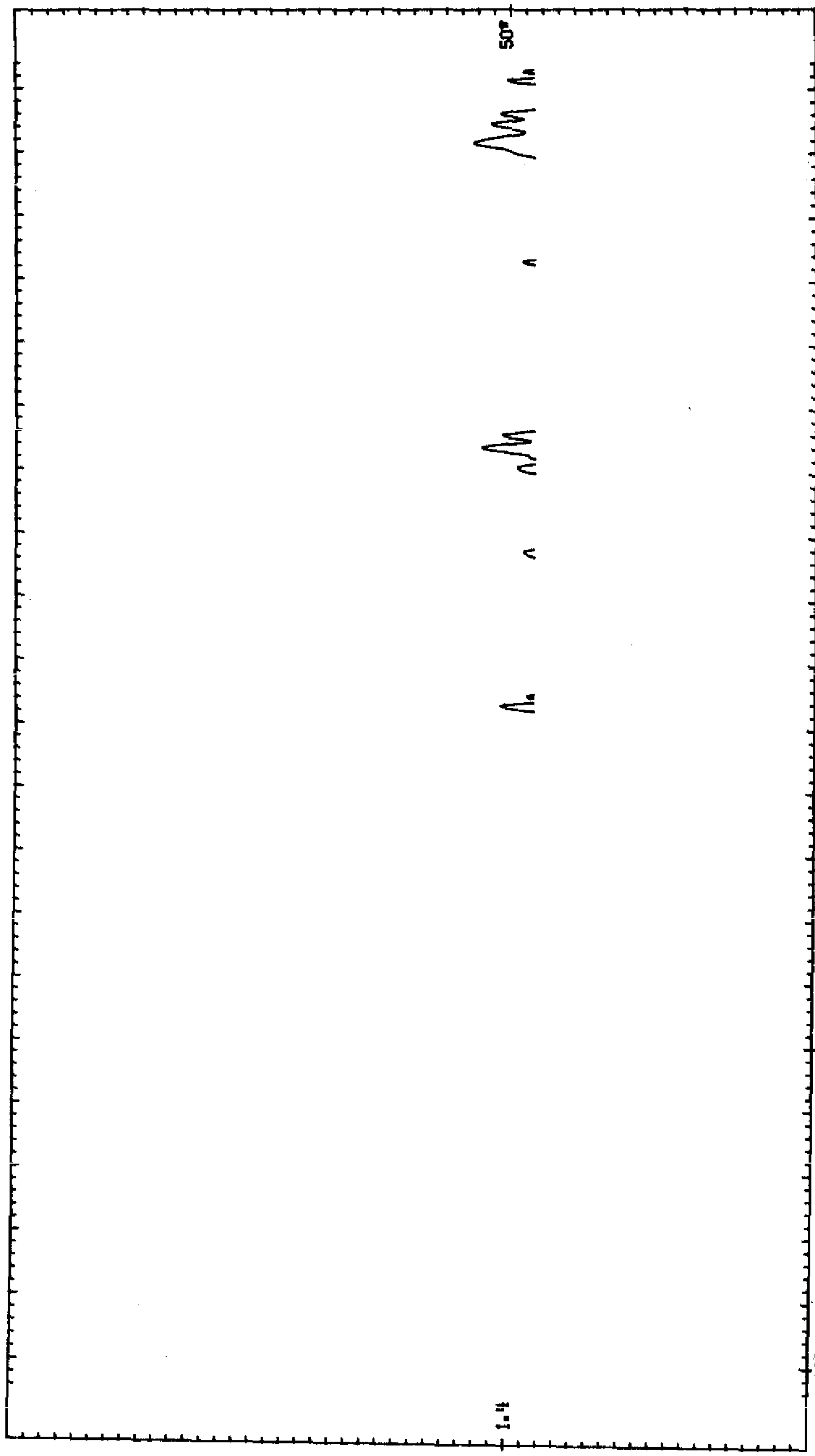
1180
1185
1190
1195
1200

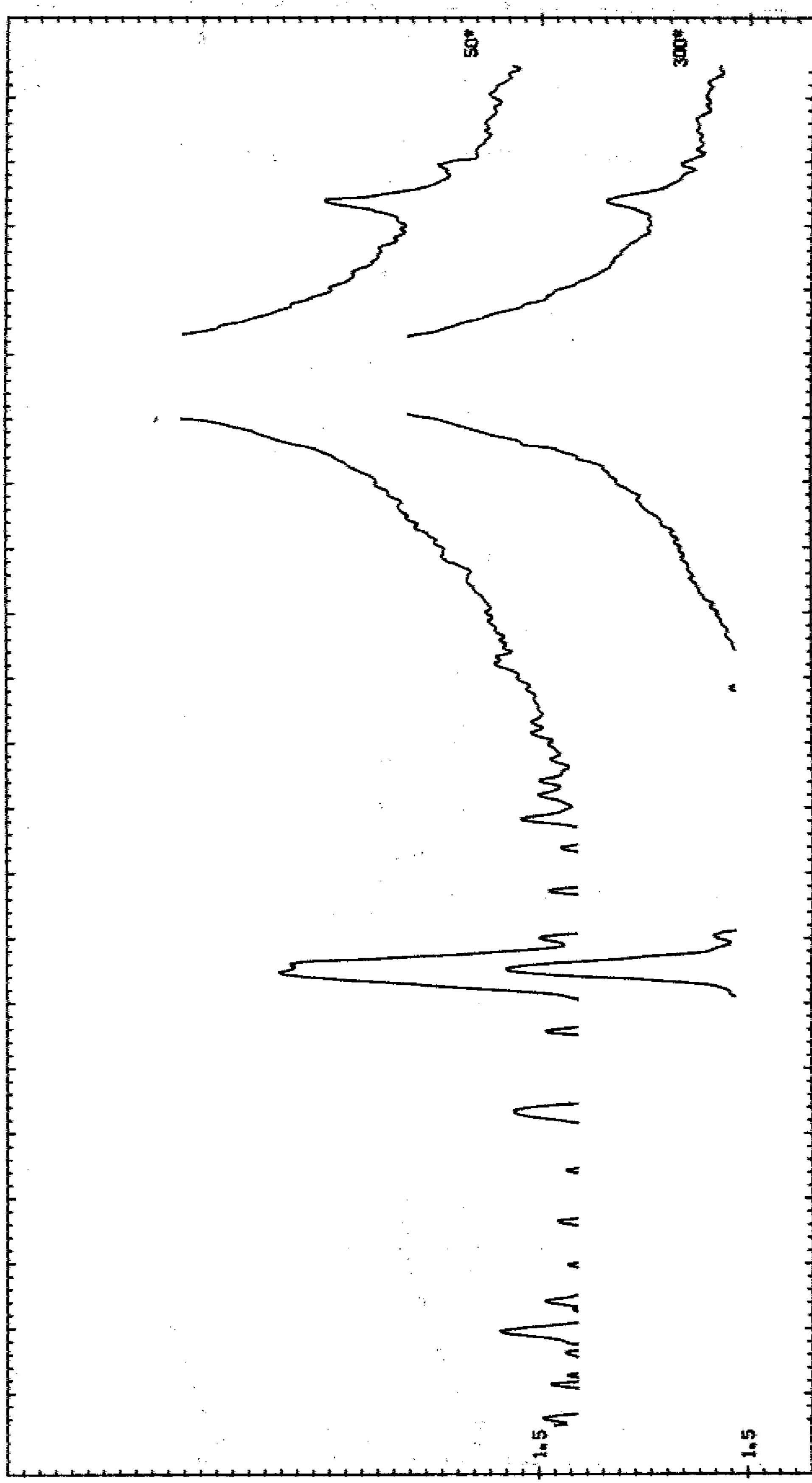
50*
300*
1.5
1.5
1200
1205
1210
1215
1220

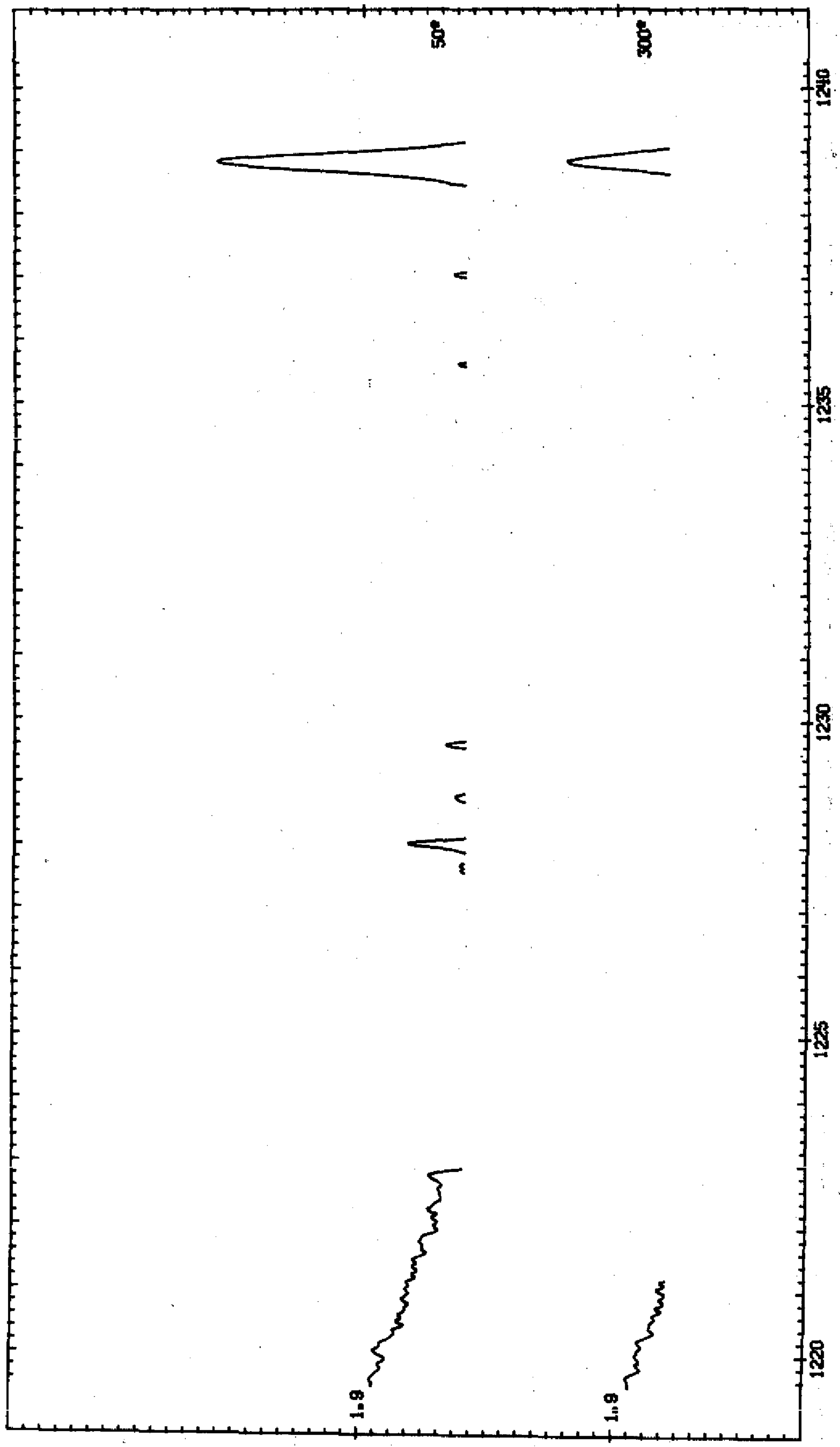
50°
300°
1.9
1.9
1220
1225
1230
1235
1240

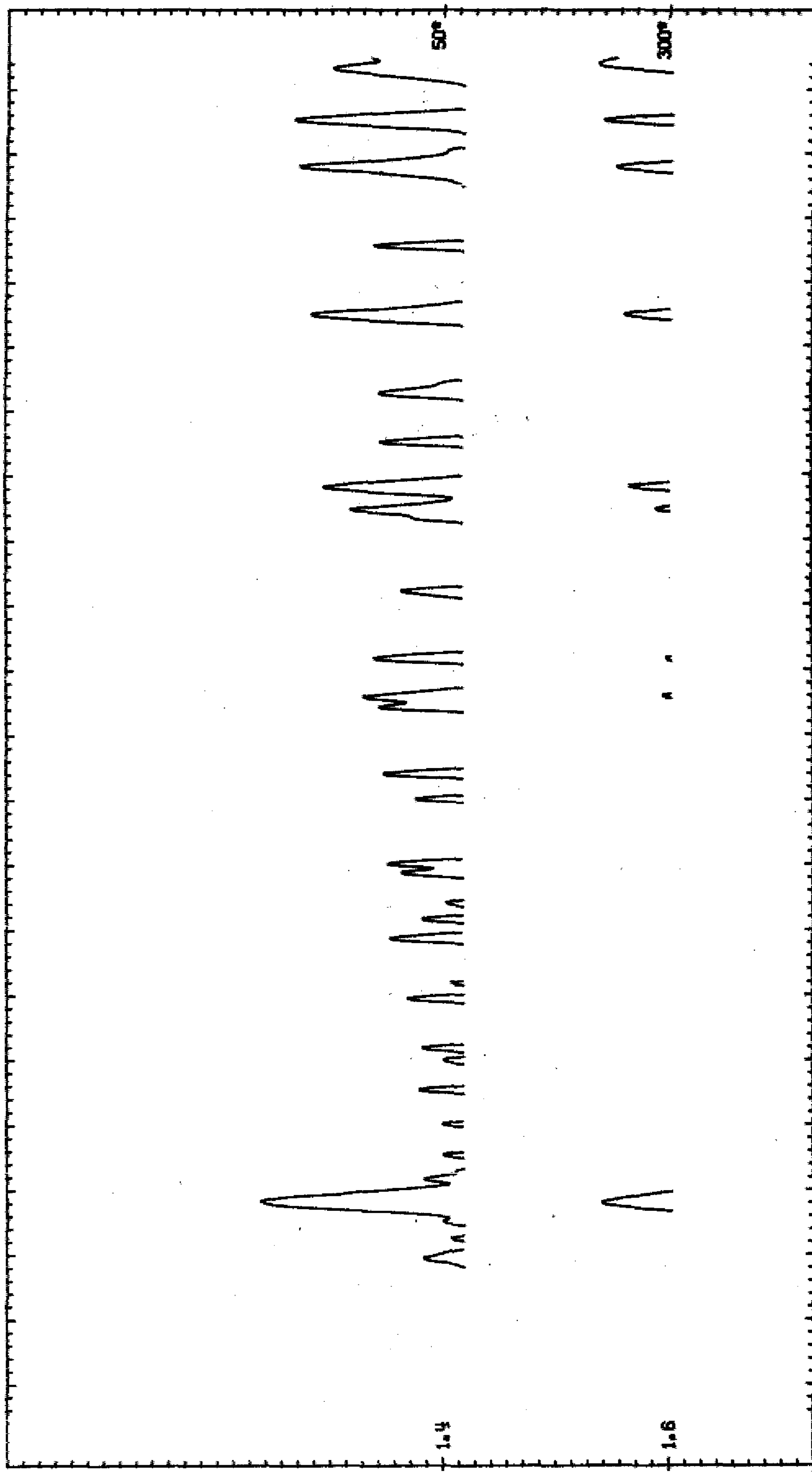
50°
300°
1260
1255
1250
1245
1240
1.4
1.6

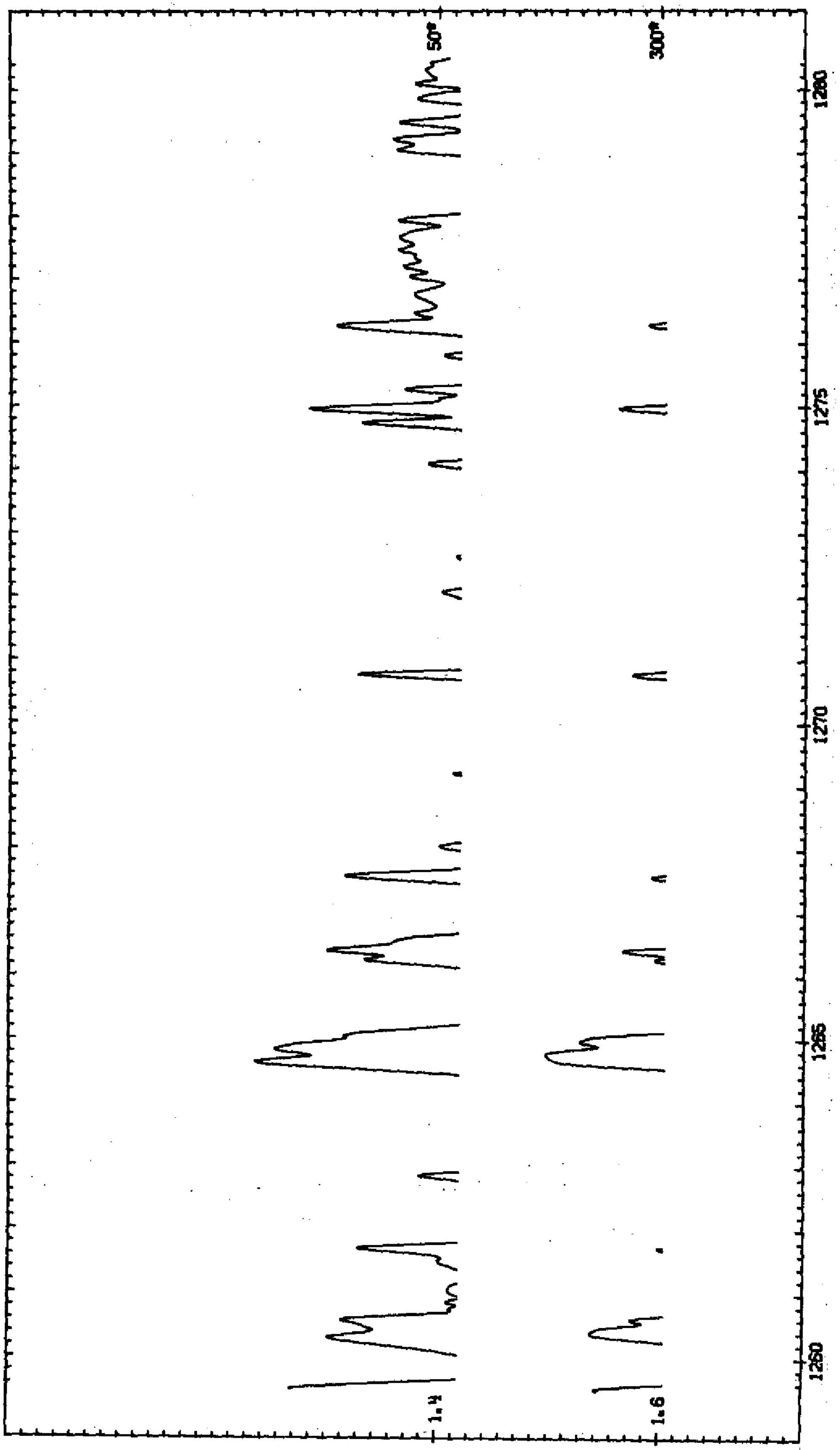
50*
300*
1280
1275
1270
1265
1260
1.4
1.6

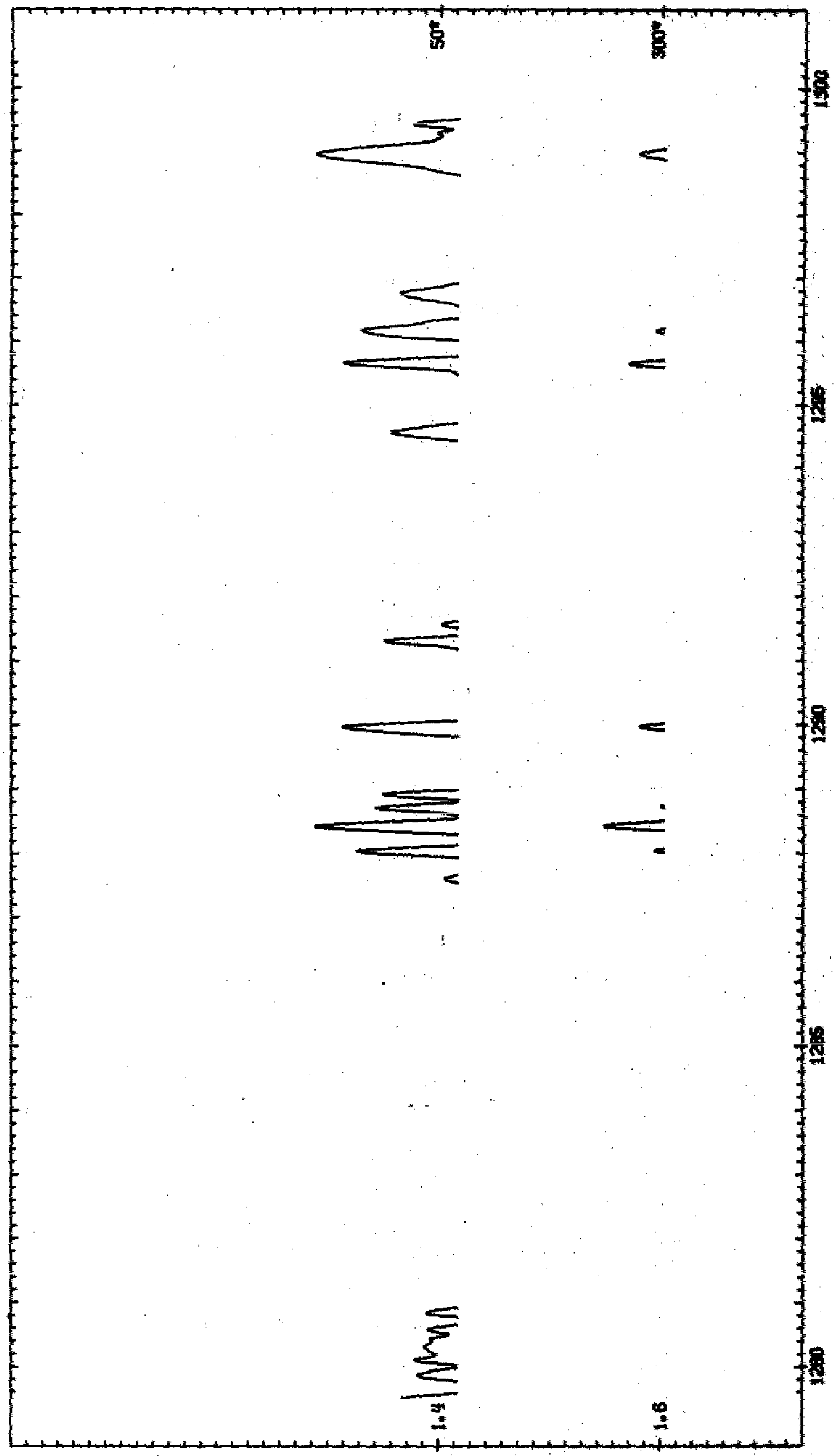

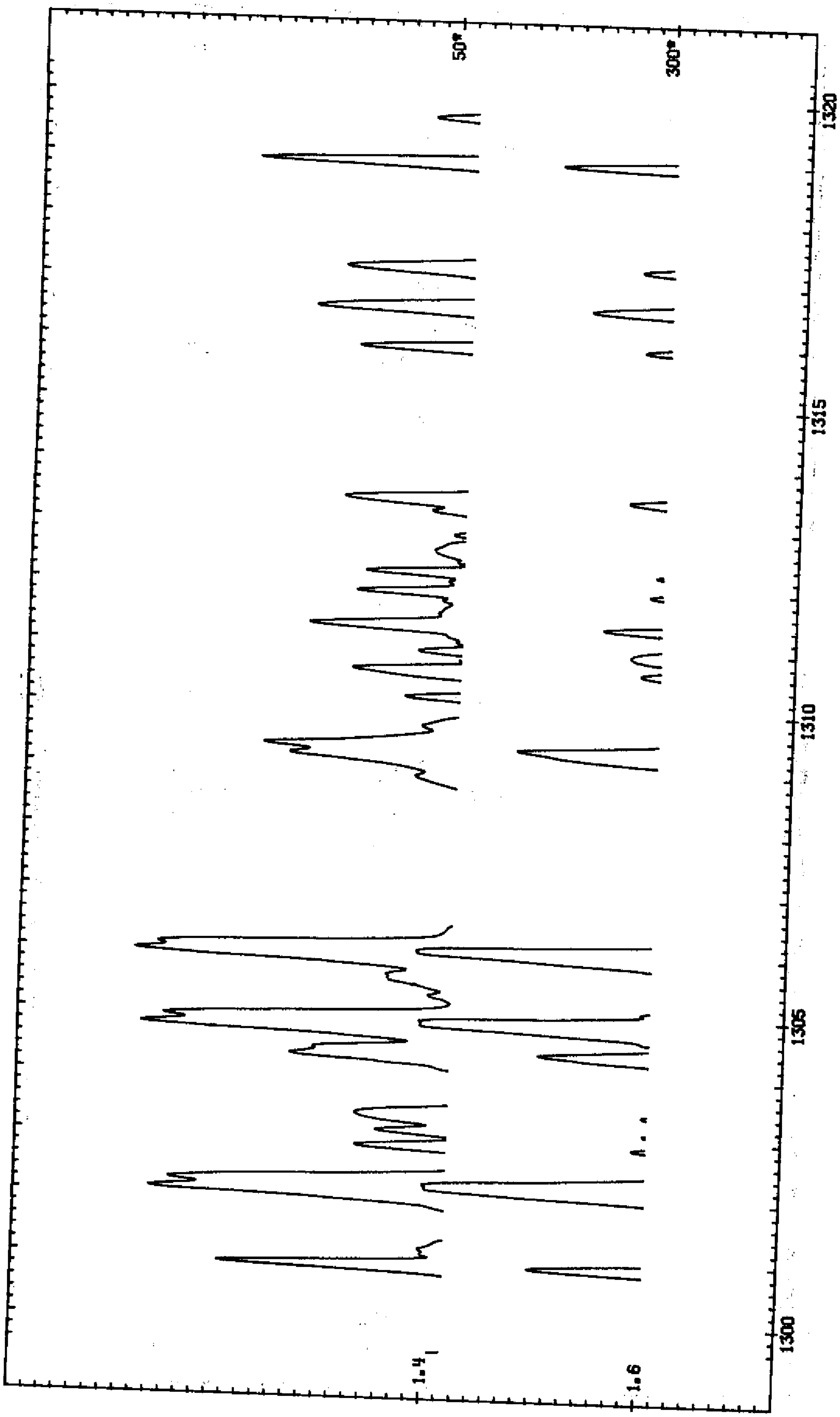
50*
300*
1.4
1.6
1300
1305
1310
1315
1320

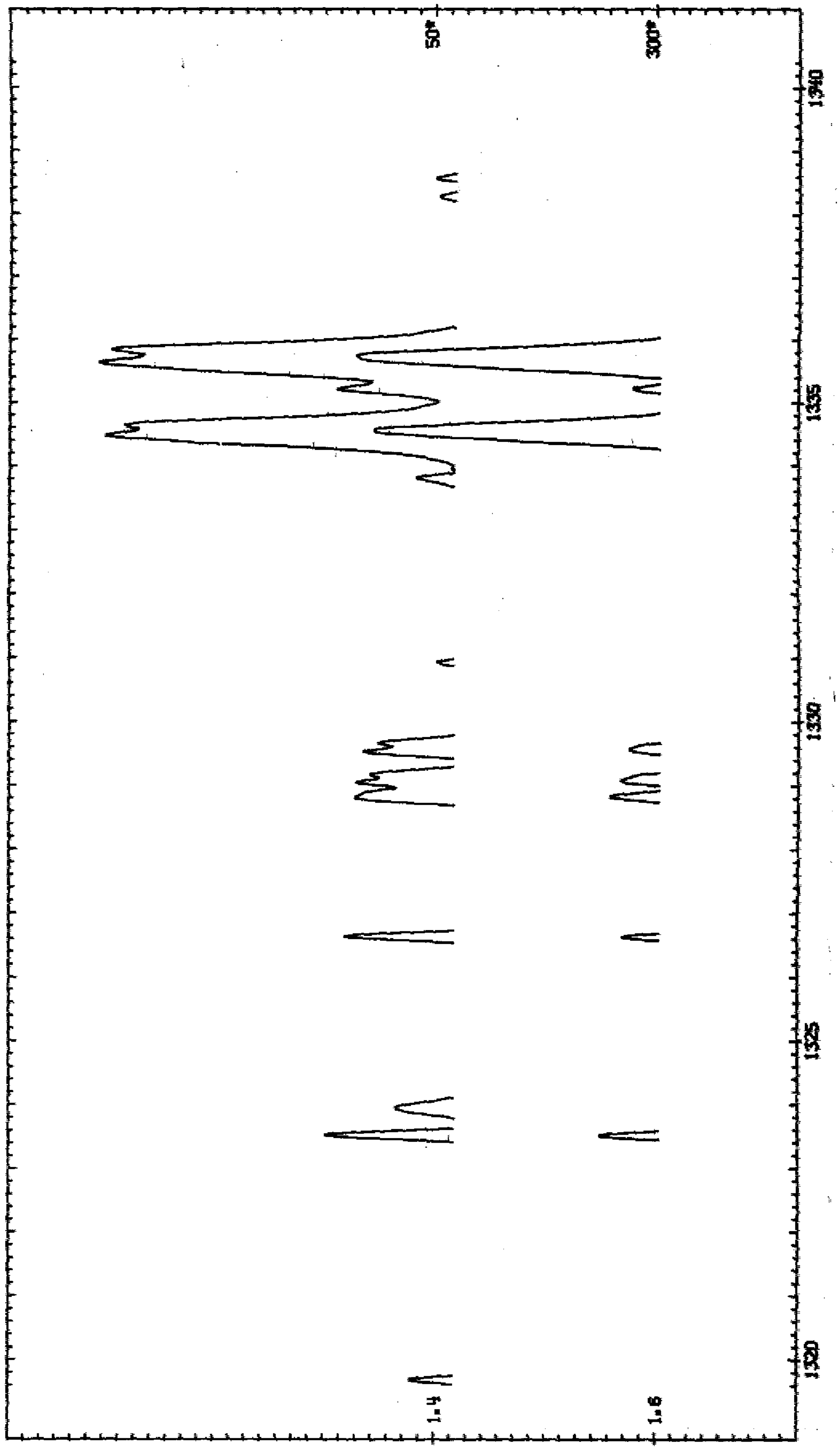
1320
1325
1330
1335
1340
1.4
1.6
50*
300*

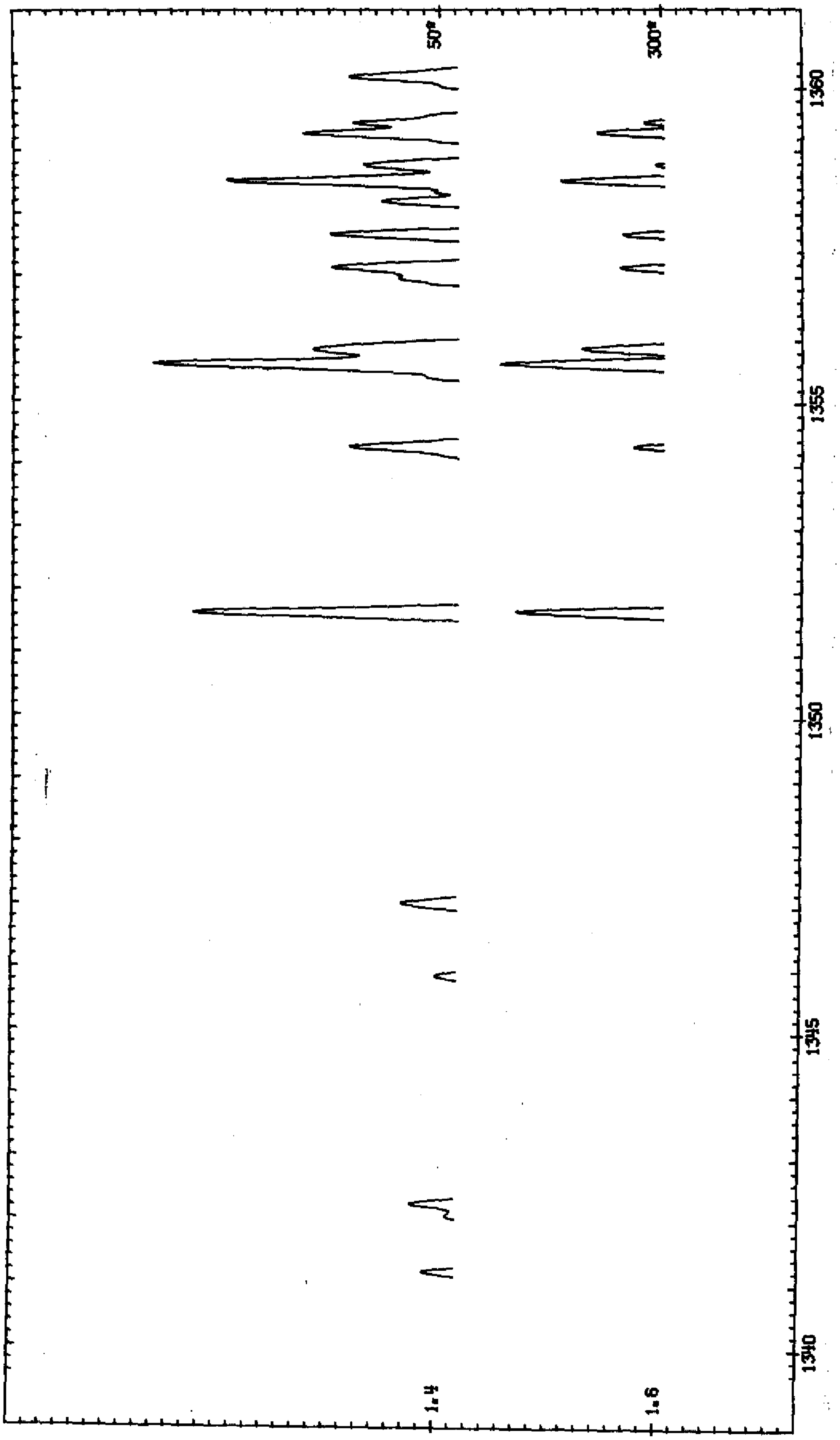
50°
300°
1360
1355
1350
1345
1340
1.4
1.6

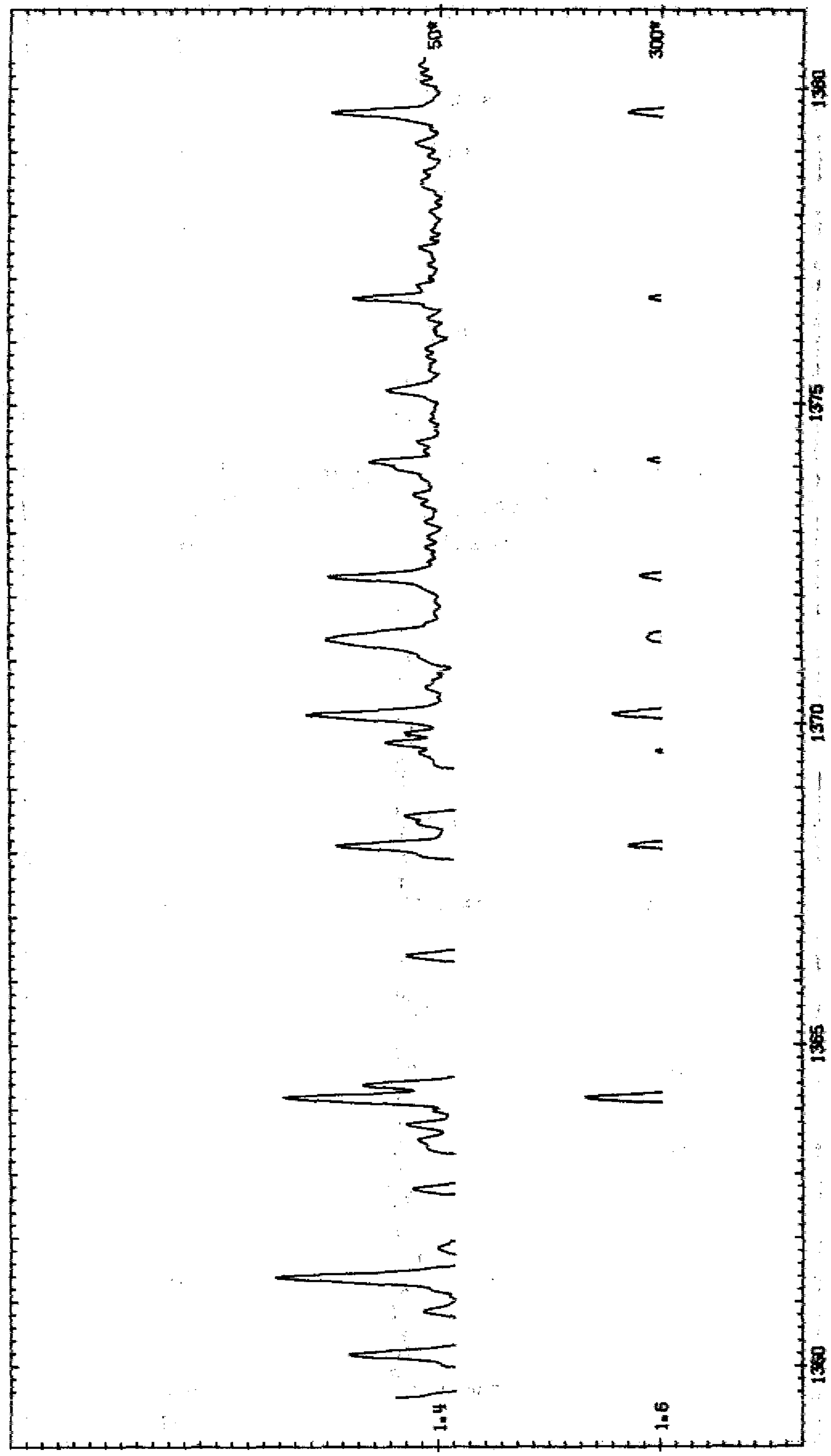
50*
300*
1360
1365
1370
1375
1380
1.4
1.6

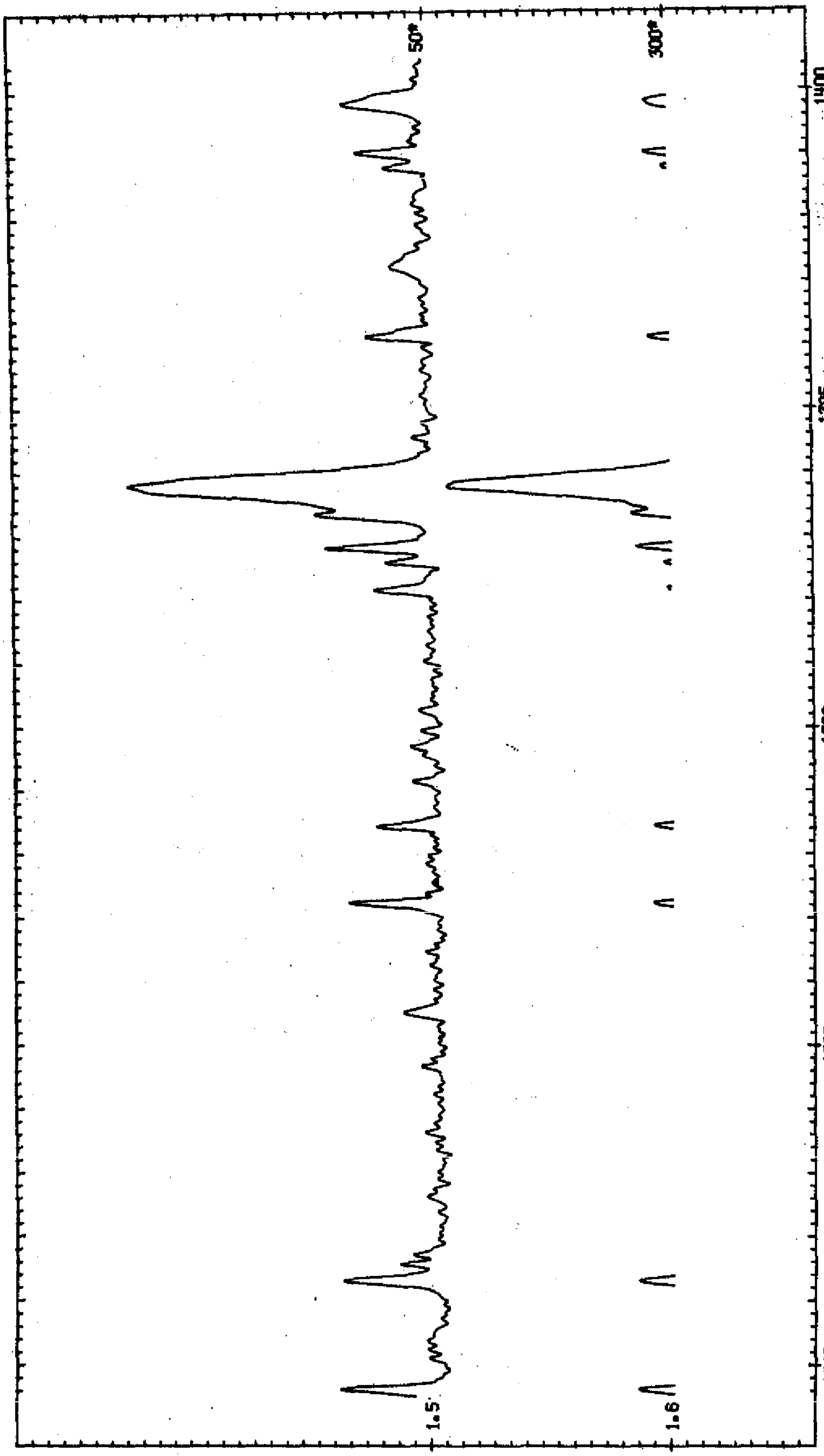
50*
300*
1400
1395
1390
1385
1380
1.5
1.6

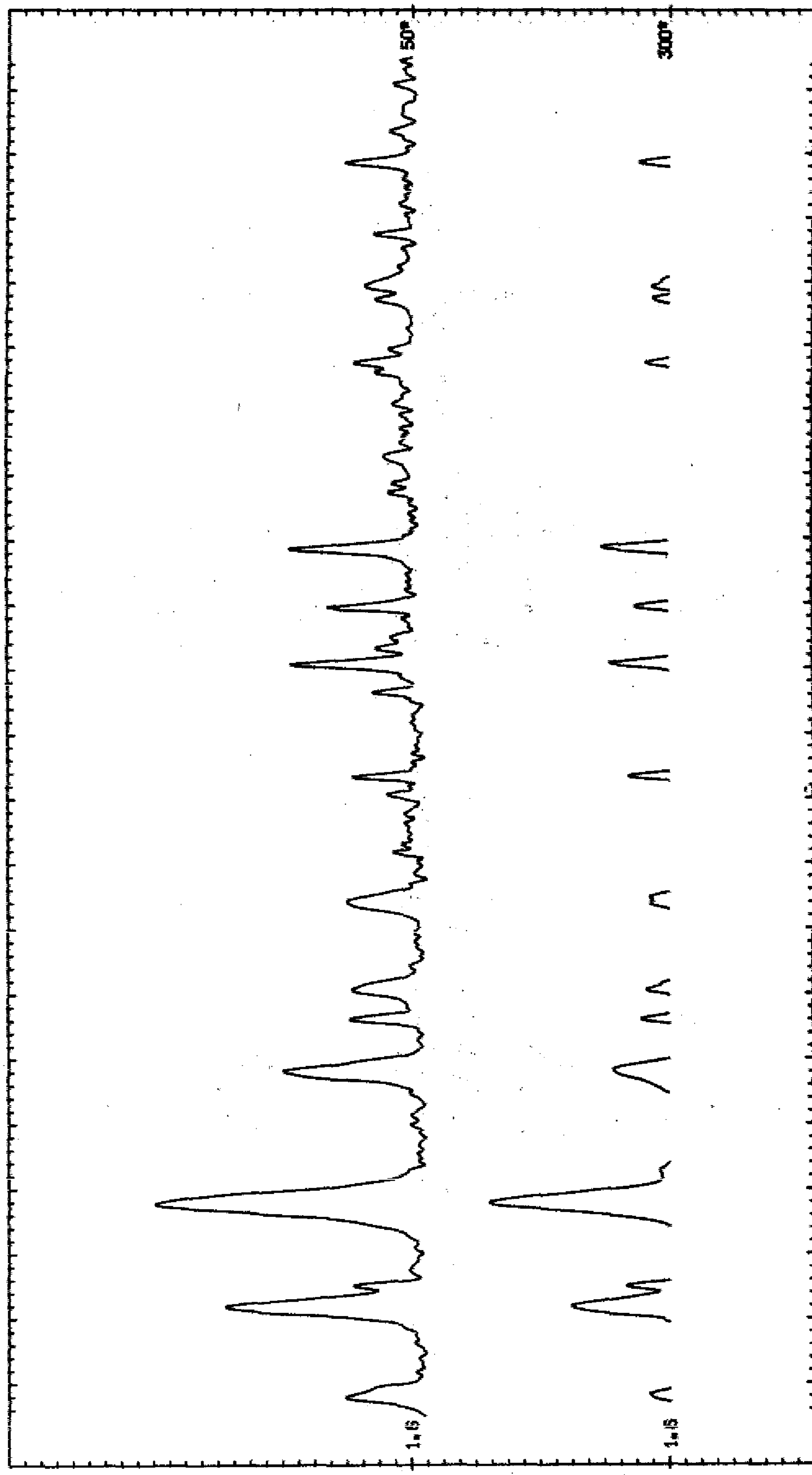

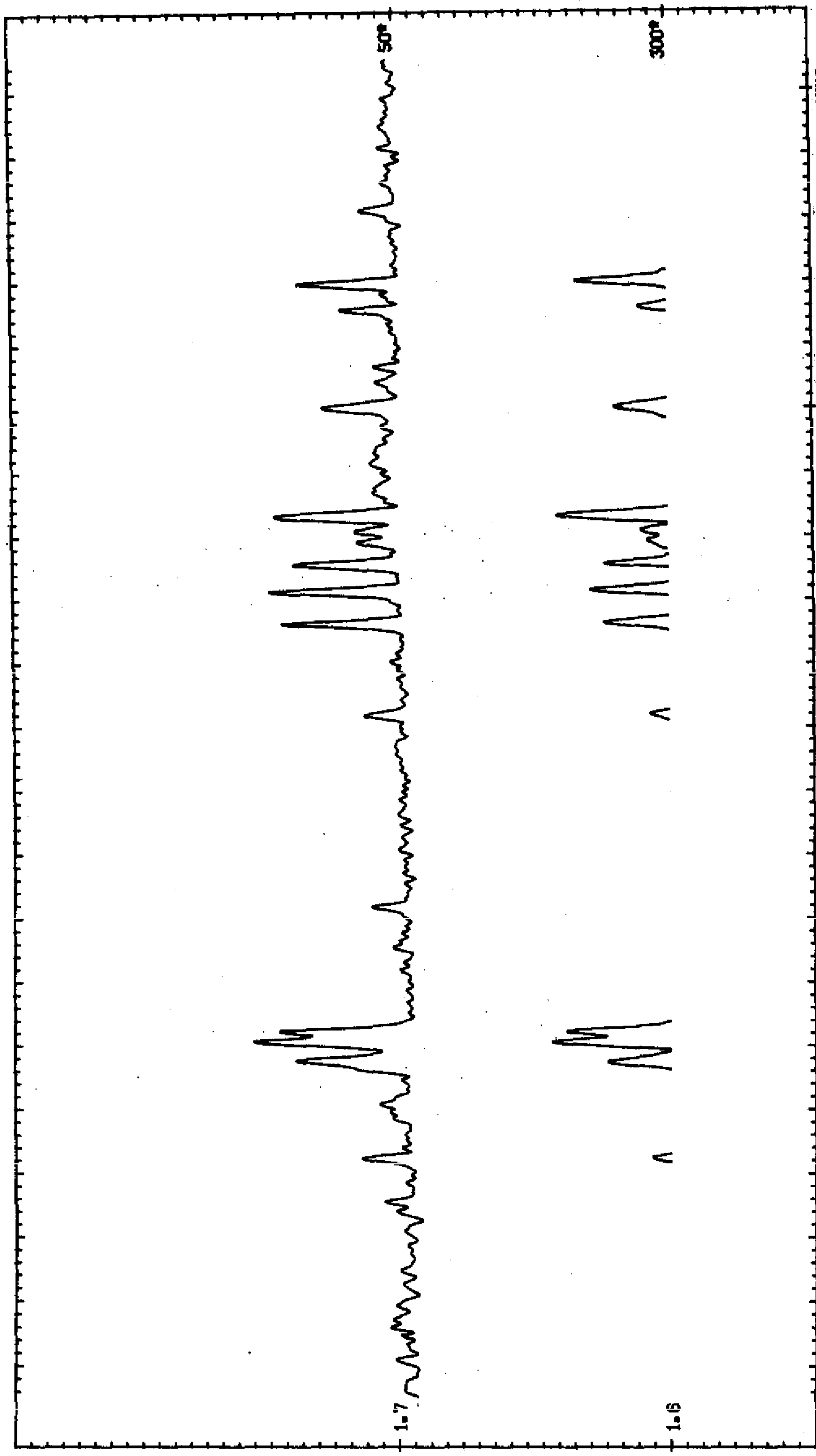
50*
300*
1440
1435
1430
1425
1420
1.7
1.6

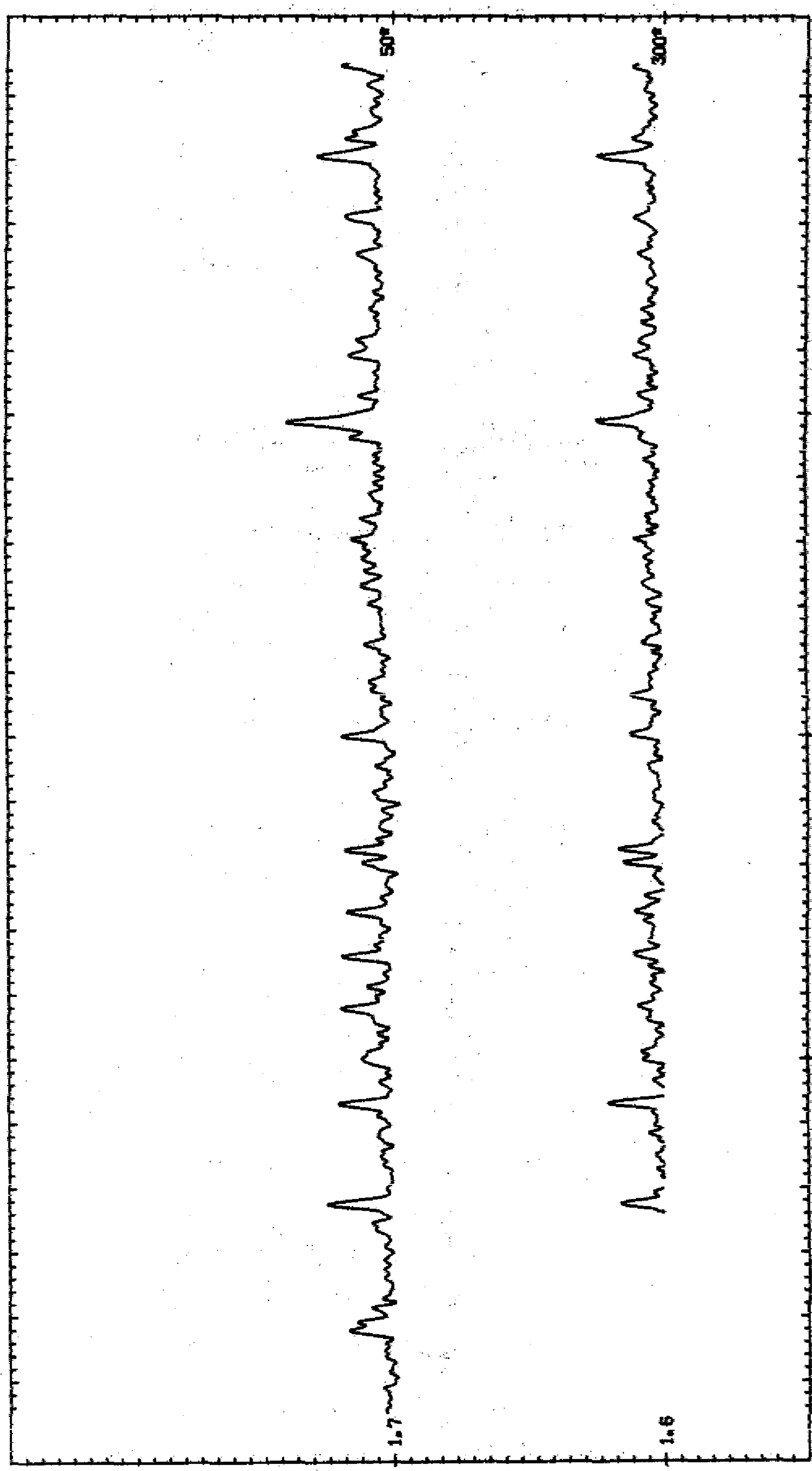
50°
300°
1.7
1.6
1940
1945
1950
1955
1960

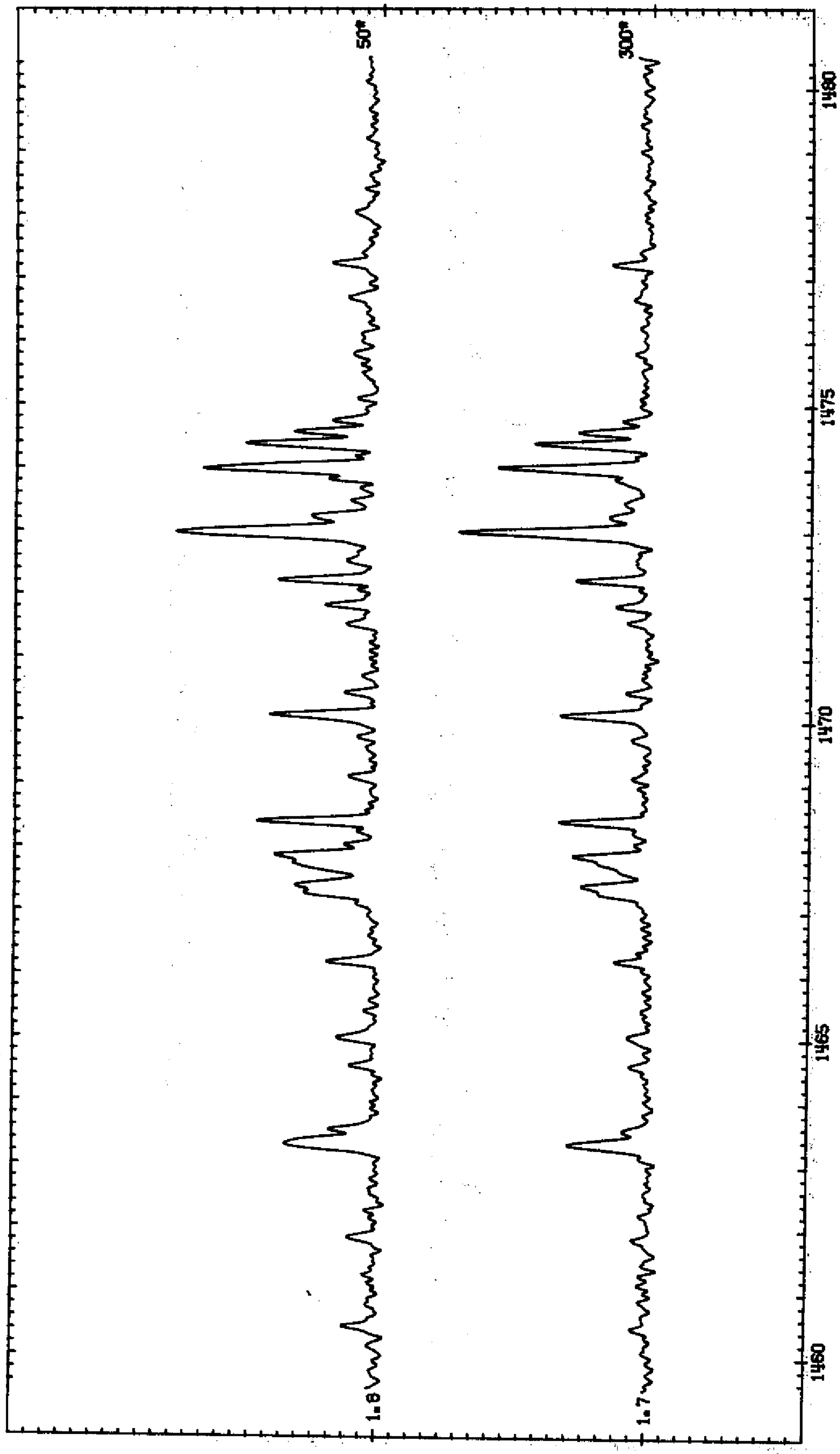
50°
300°
1480
1475
1470
1465
1460
1.8
1.7

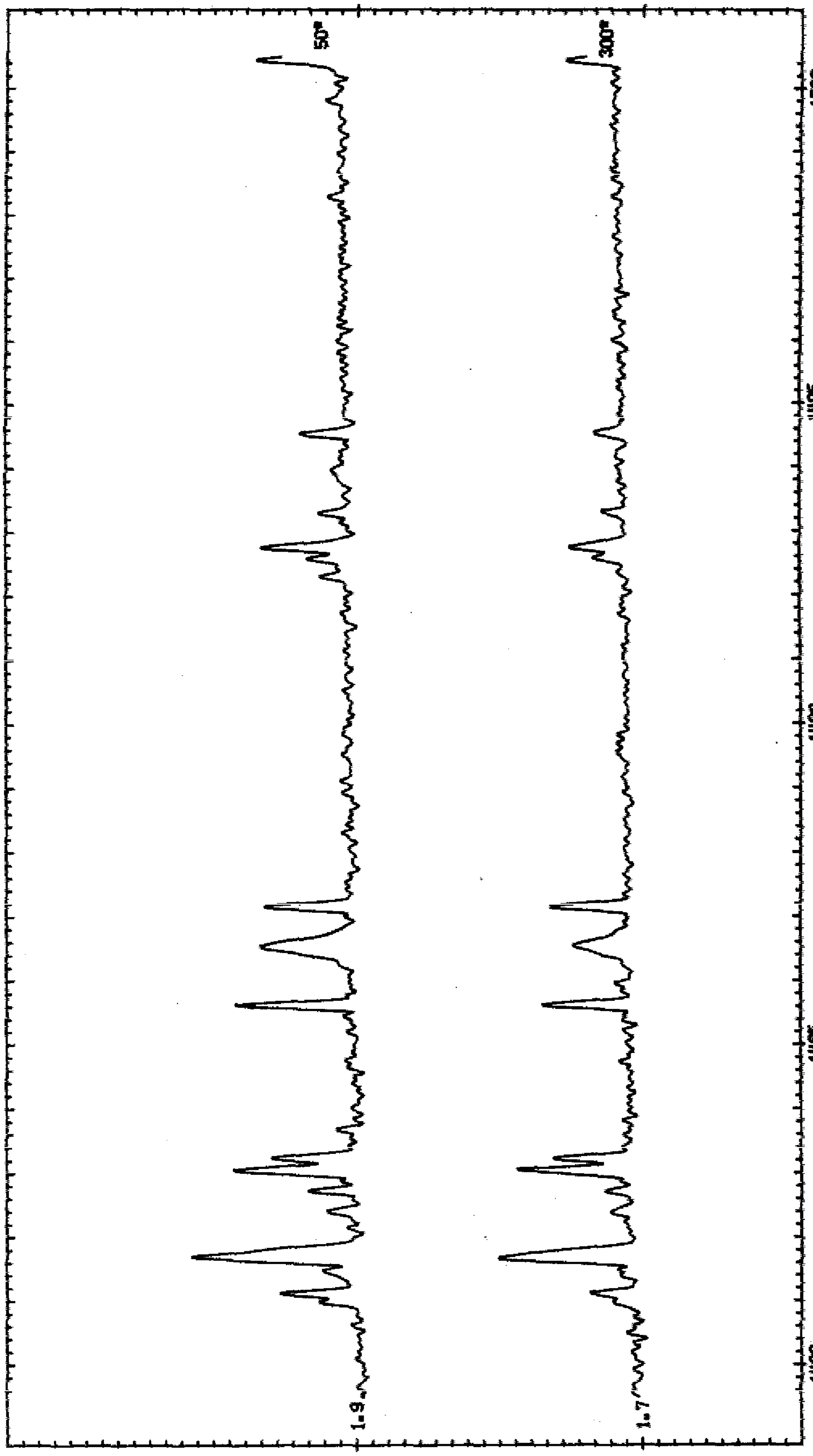
50°
300°
1.9
1.7
1480
1485
1490
1495
1500

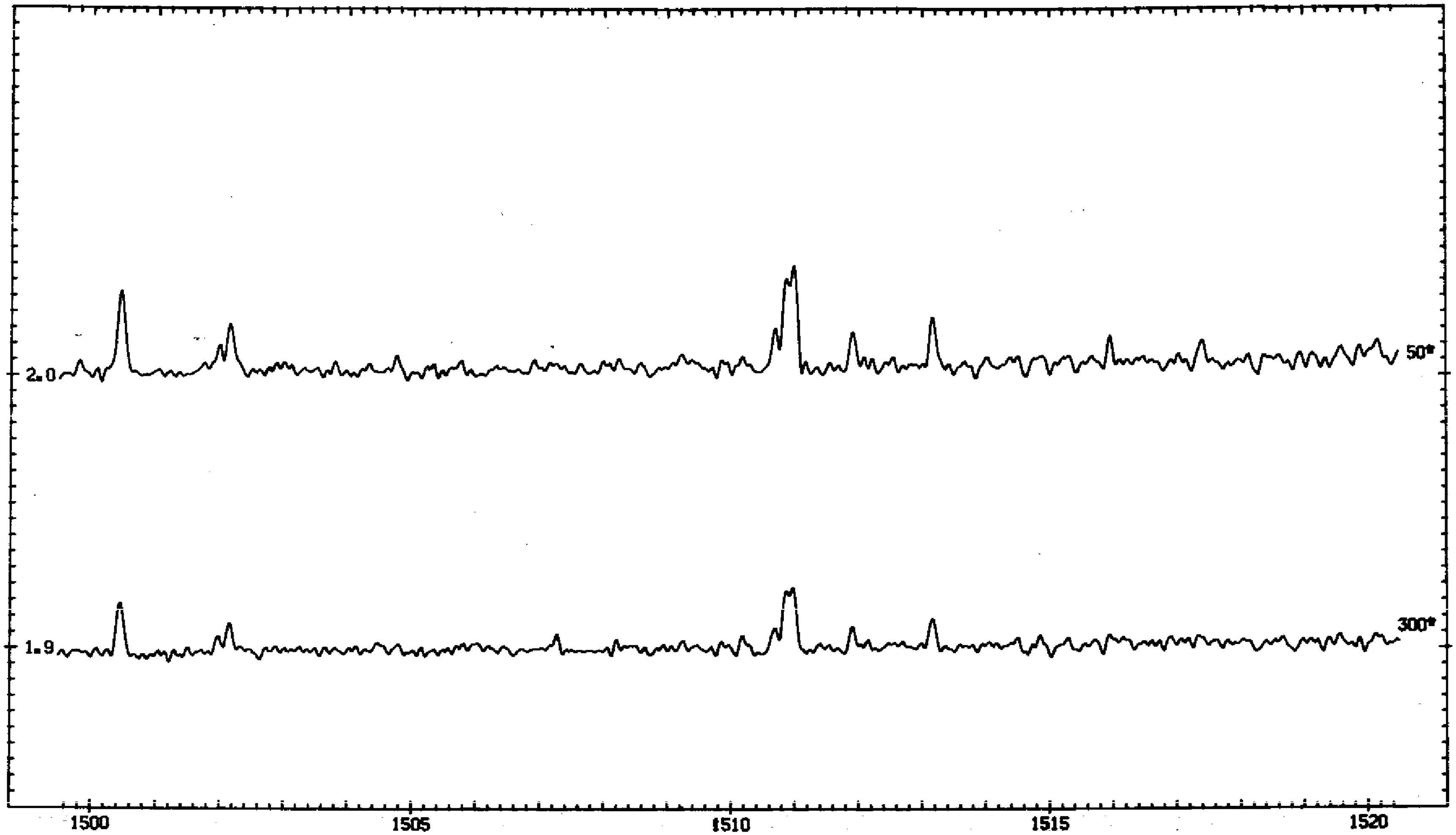
2.0
1.9
50*
300*
1500
1505
1510
1515
1520

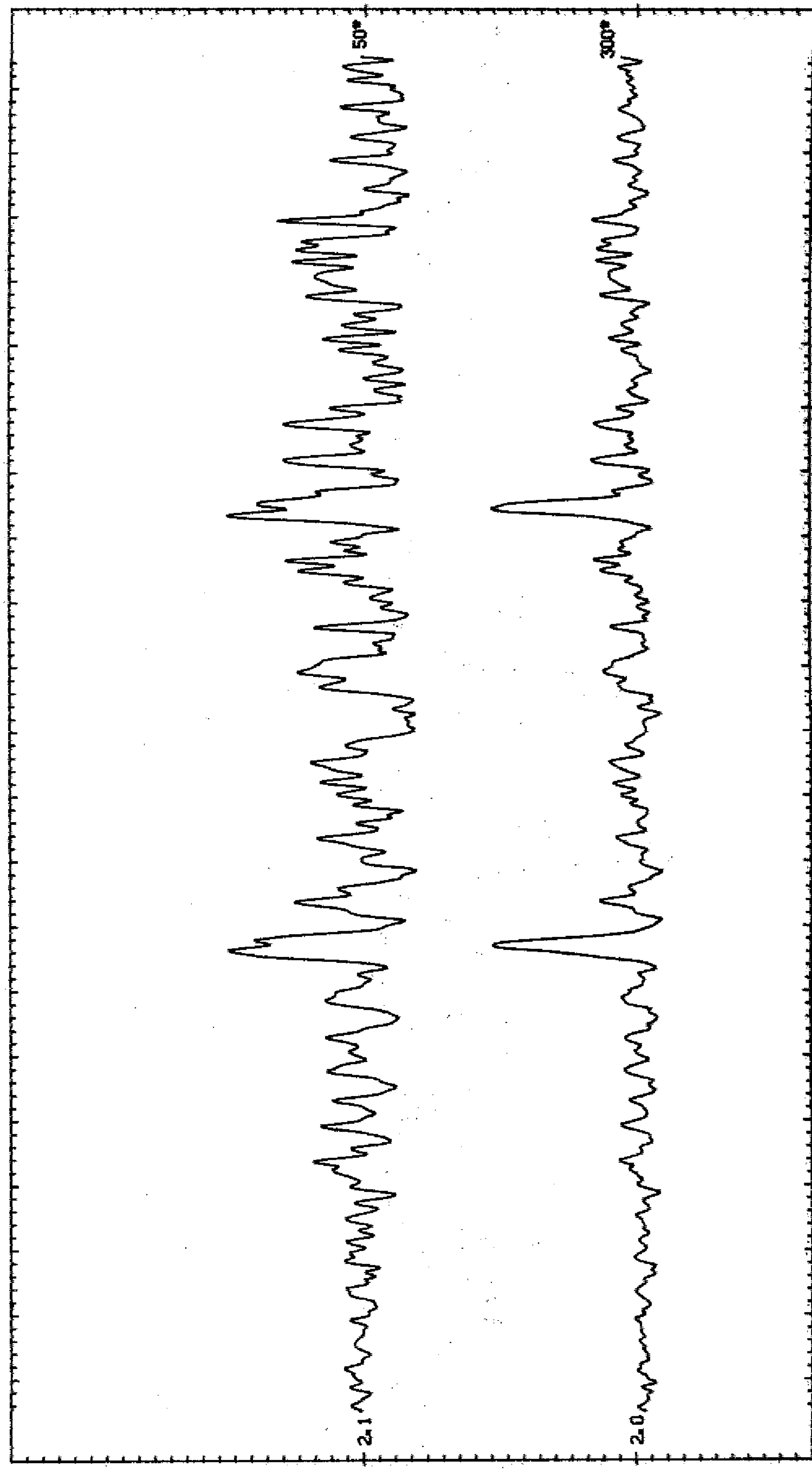
50*
300*
2.1
2.0
1520
1525
1530
1535
1540

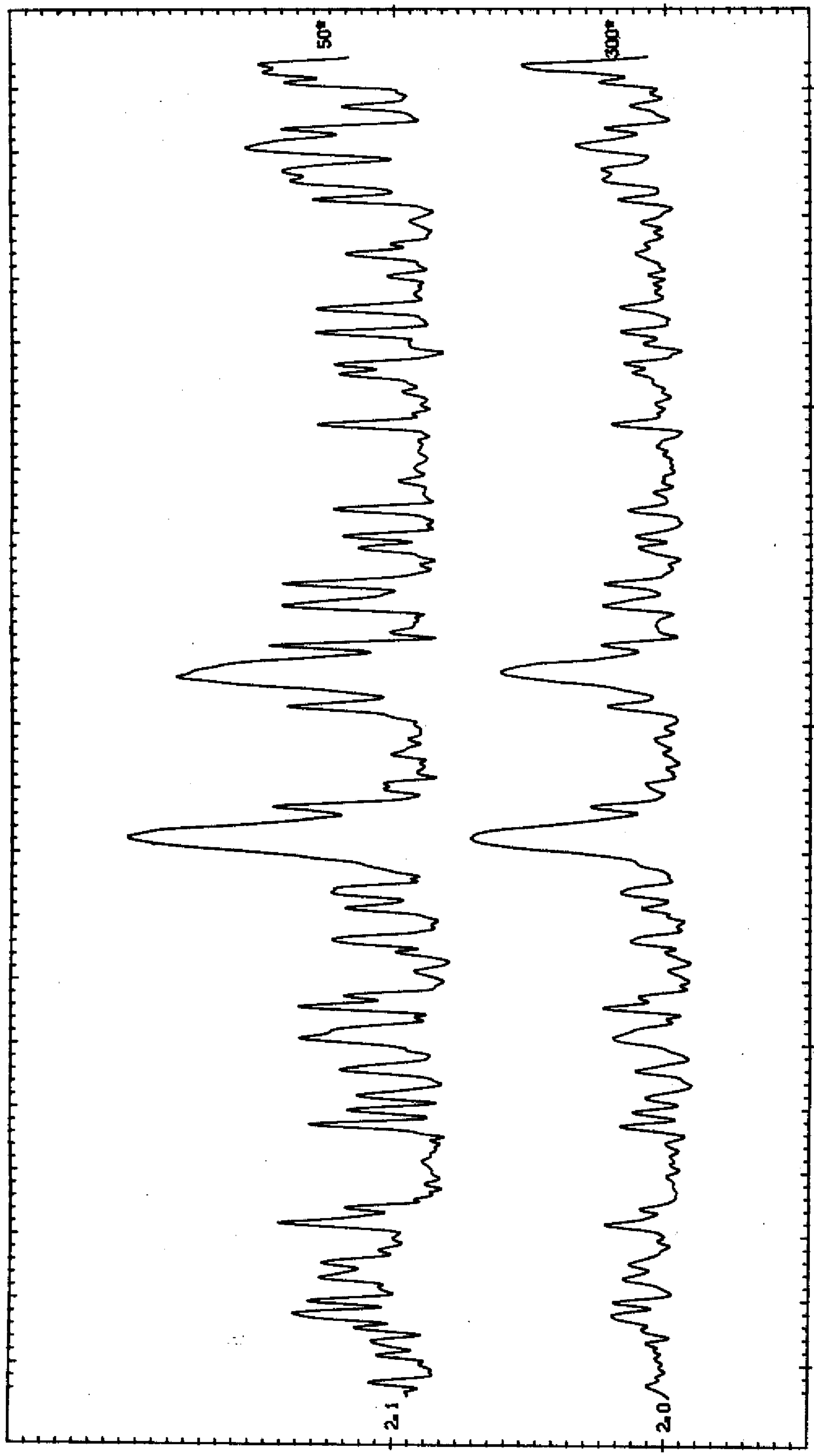

50*
300*
1560
1555
1550
1545
1540
2.1
2.0

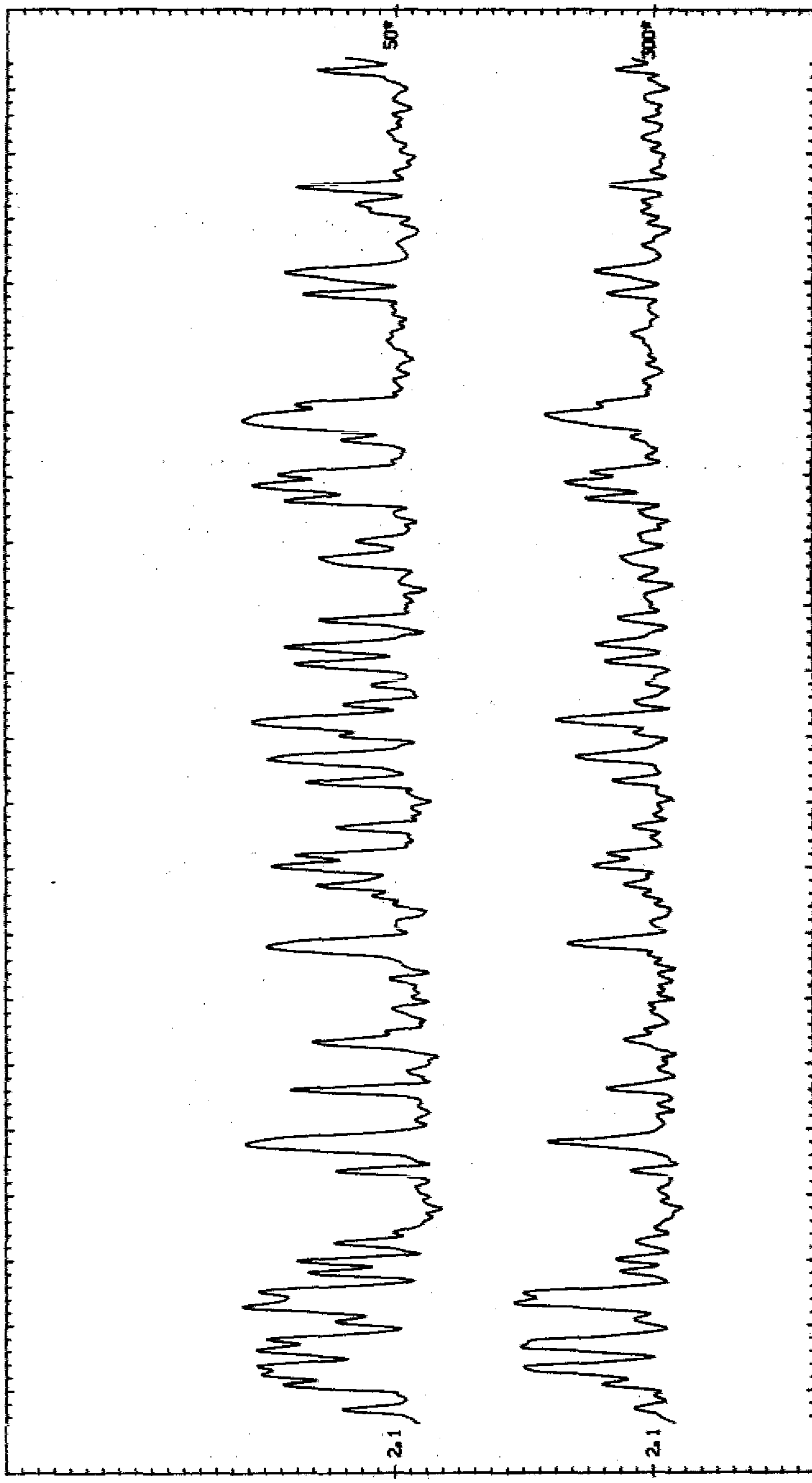
50*
300*
2.1
2.1
1560
1565
1570
1575
1580

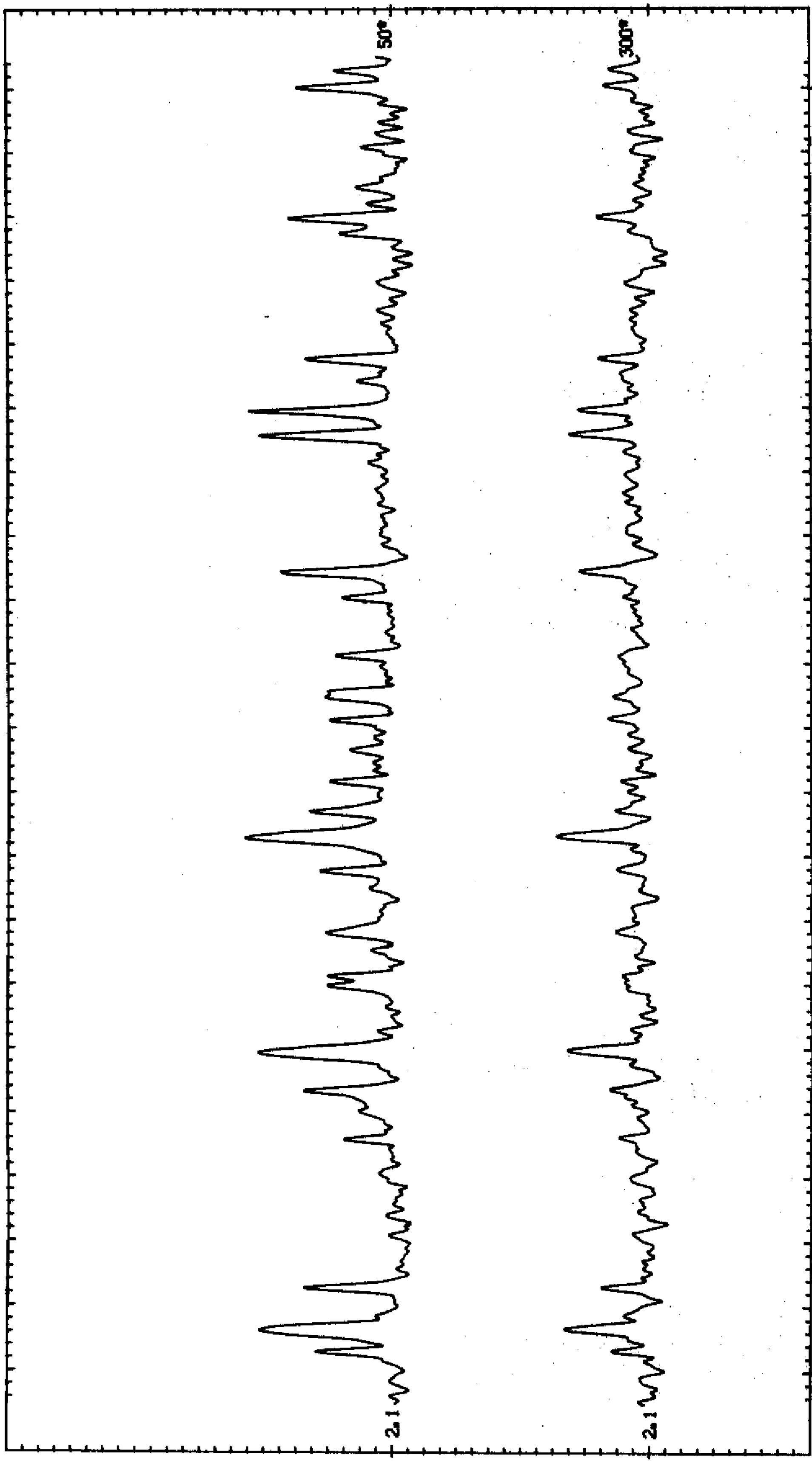

1580
1585
1590
1595
1600
2.1
50°
2.1
300°

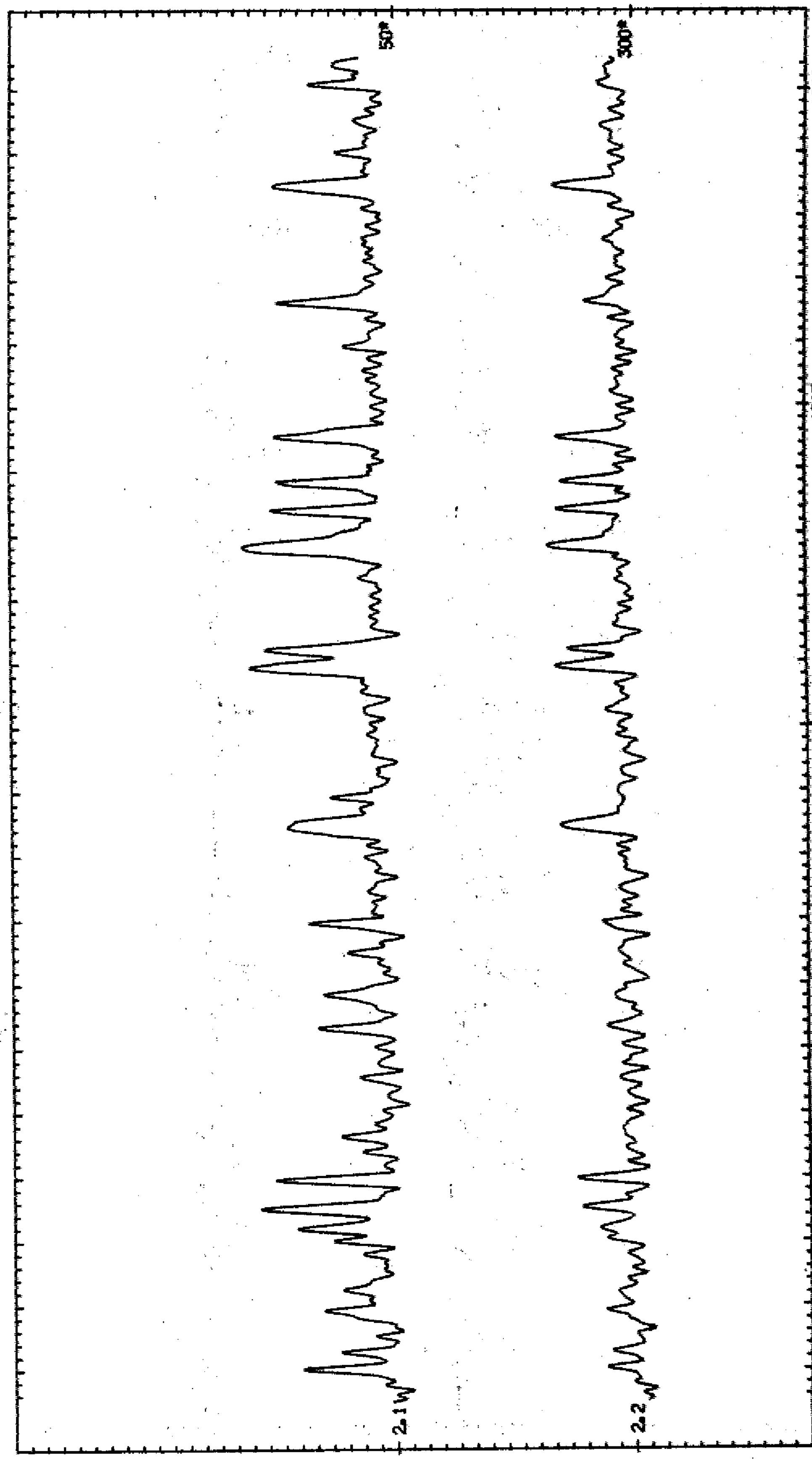
1600
1605
1610
1615
1620
2.1W
2.2
50*
300*

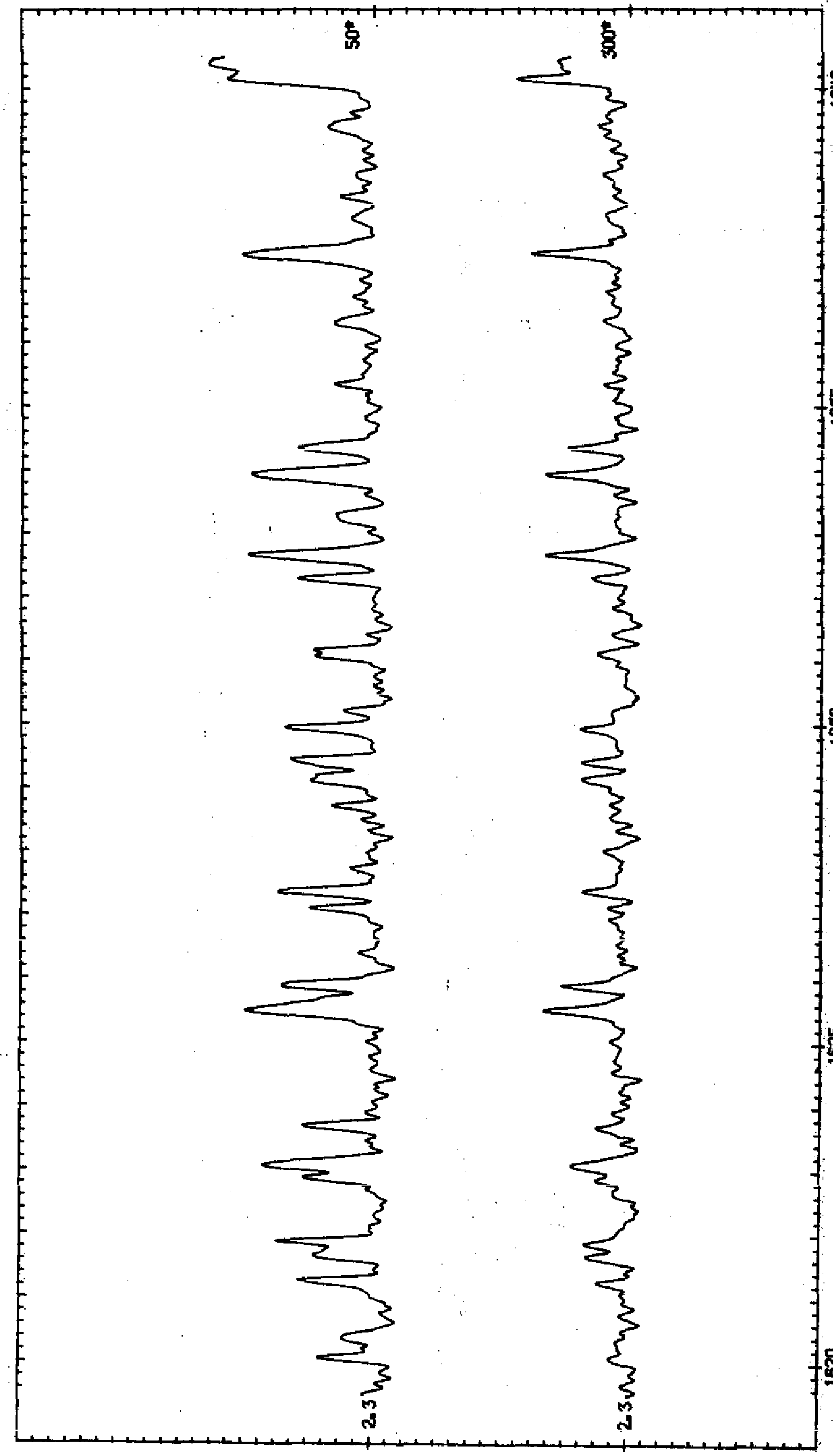
50*
300*
1640
1635
1630
1625
1620
2.3
2.3

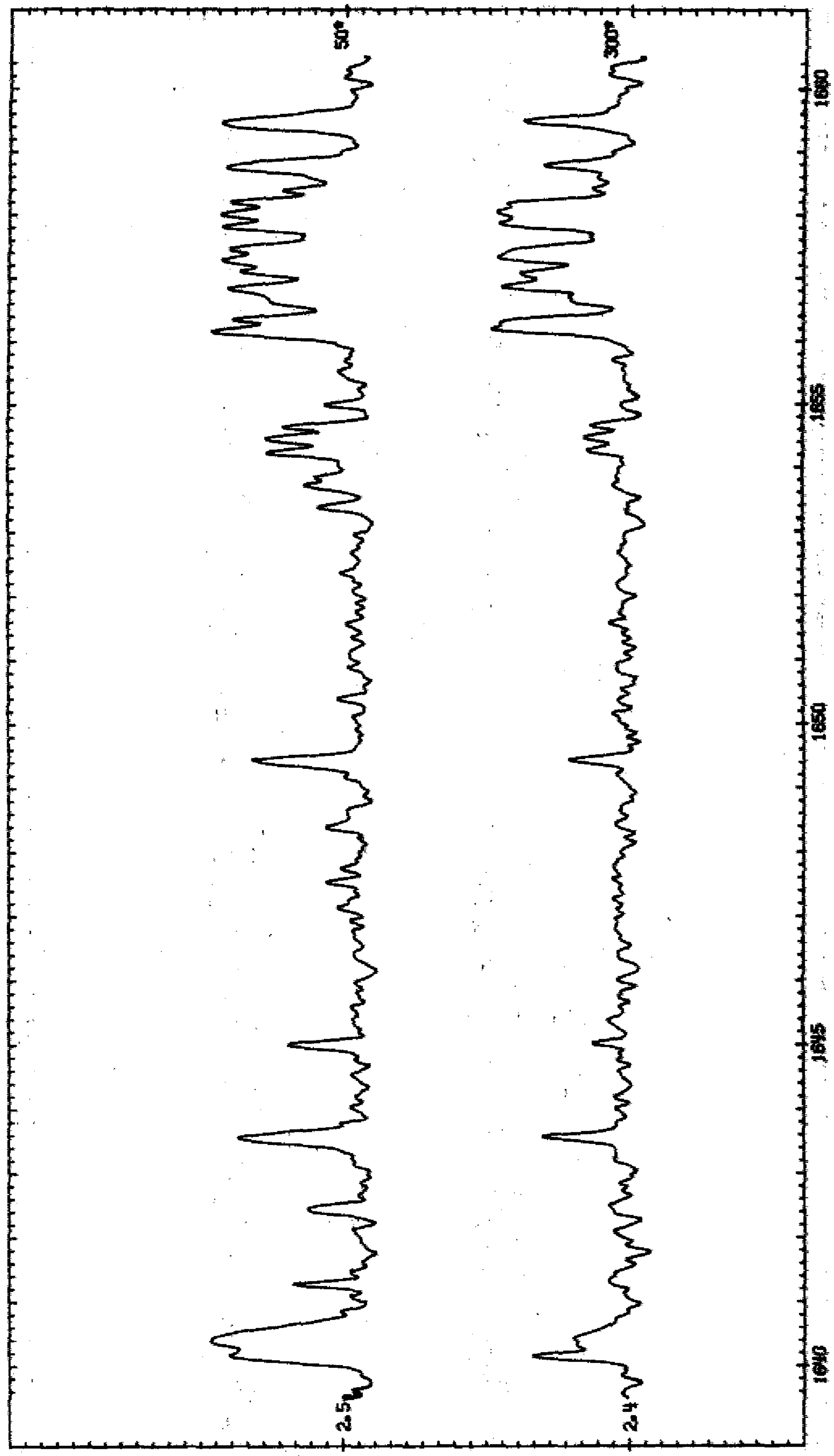
50°
300°
1660
1655
1650
1645
1640
2.5
2.4

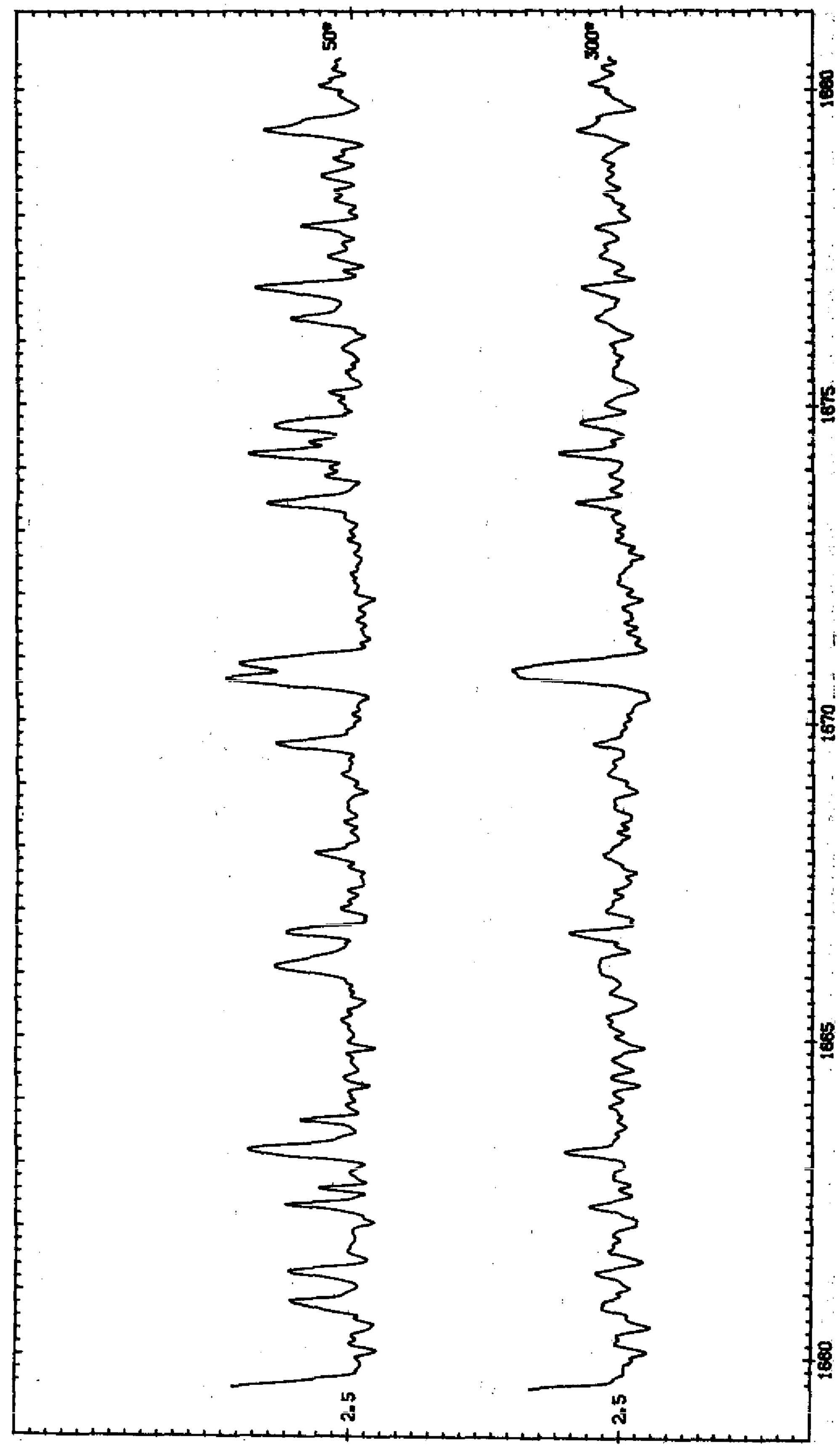
50°
300°
2.5
2.5
1660
1665
1670
1675
1680

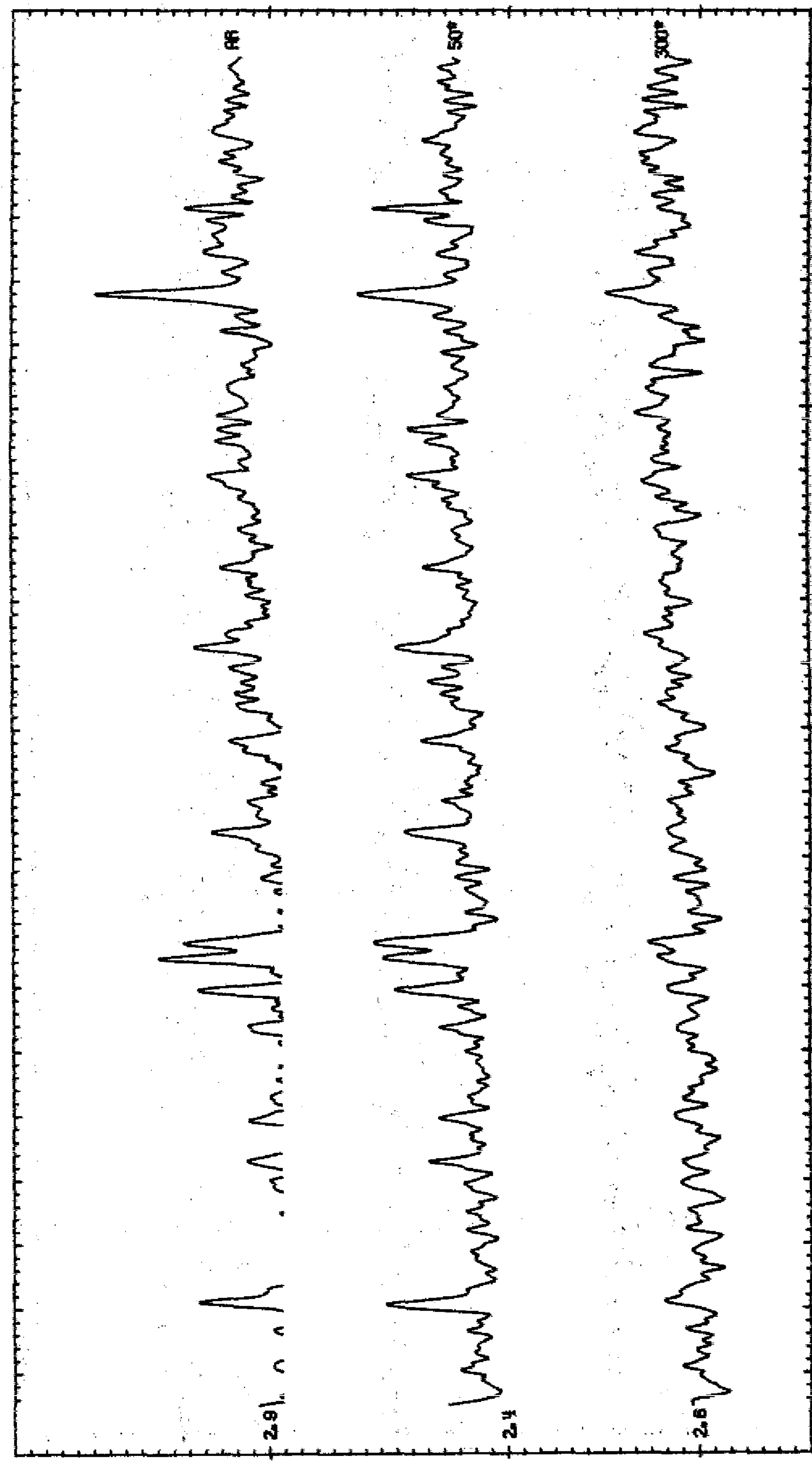

AR
50°
300°
2.9
2.4
2.6
1680
1685
1690
1695
1700

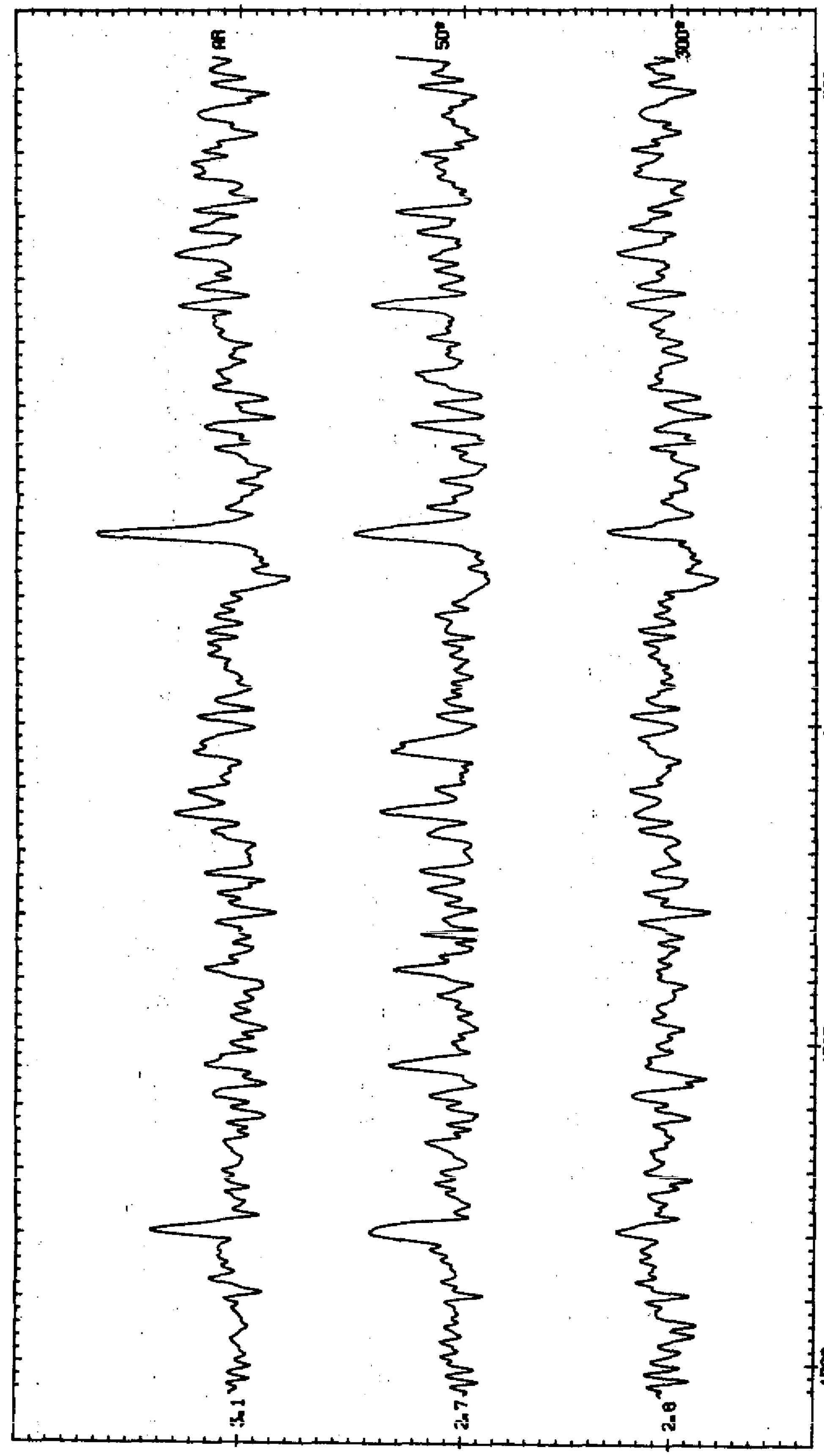
AR
50°
300°
3.1
2.7
2.8
1700
1705
1710
1715
1720

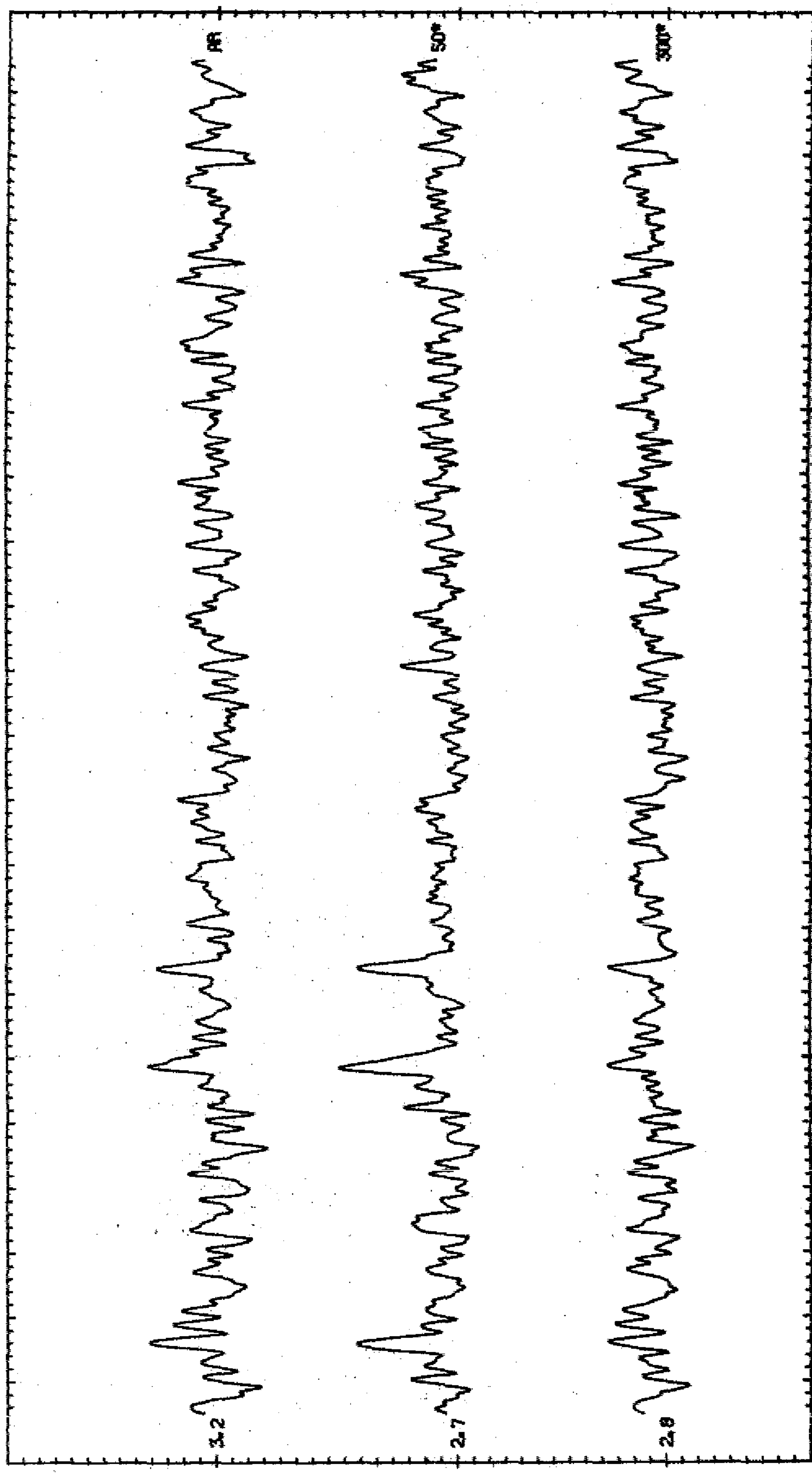
AR
50°
300°
3.2
2.7
2.8
1720
1725
1730
1735
1740

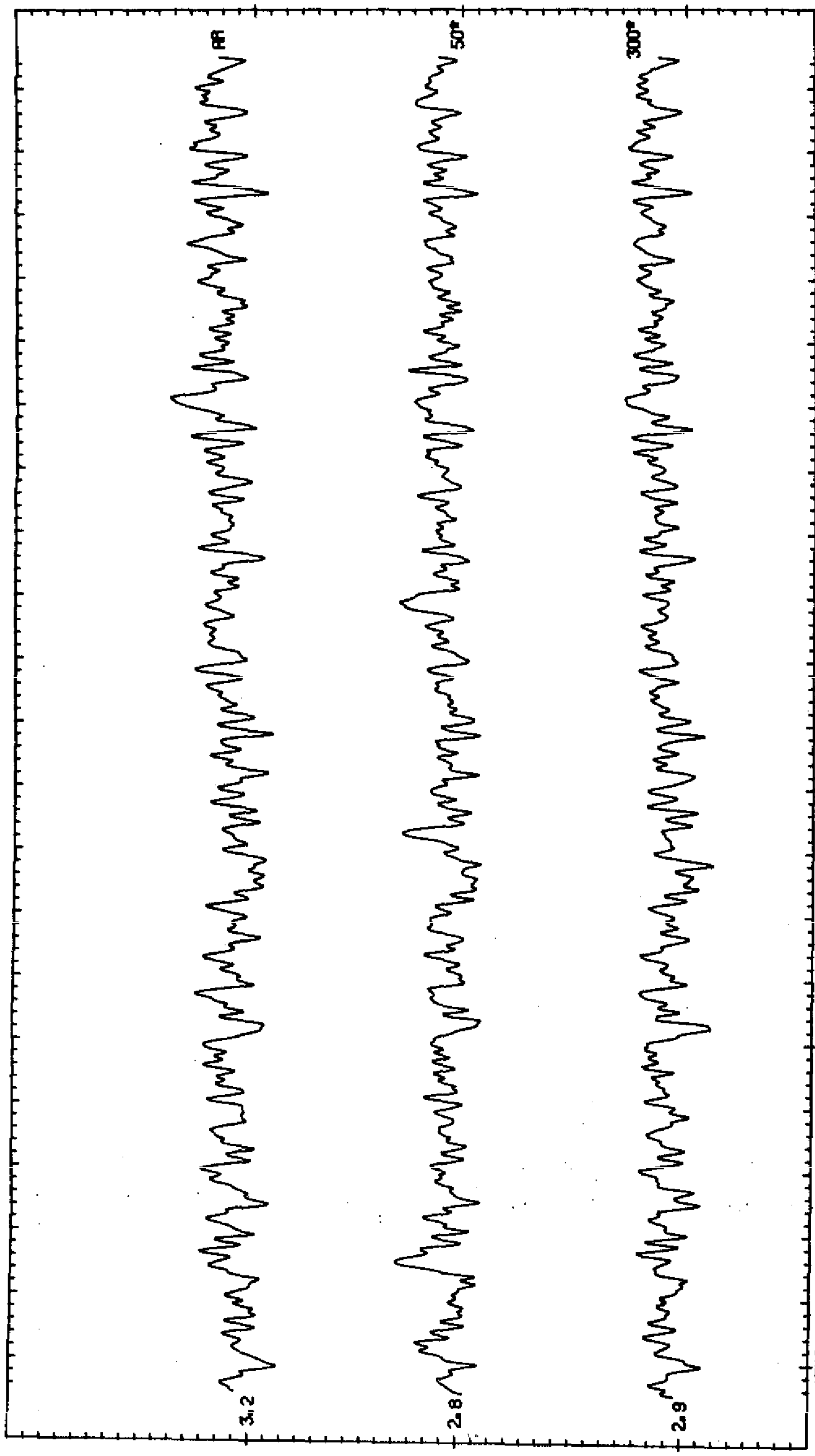
AA
50°
300°
1760
1755
1750
1745
1740
3.2
2.8
2.9

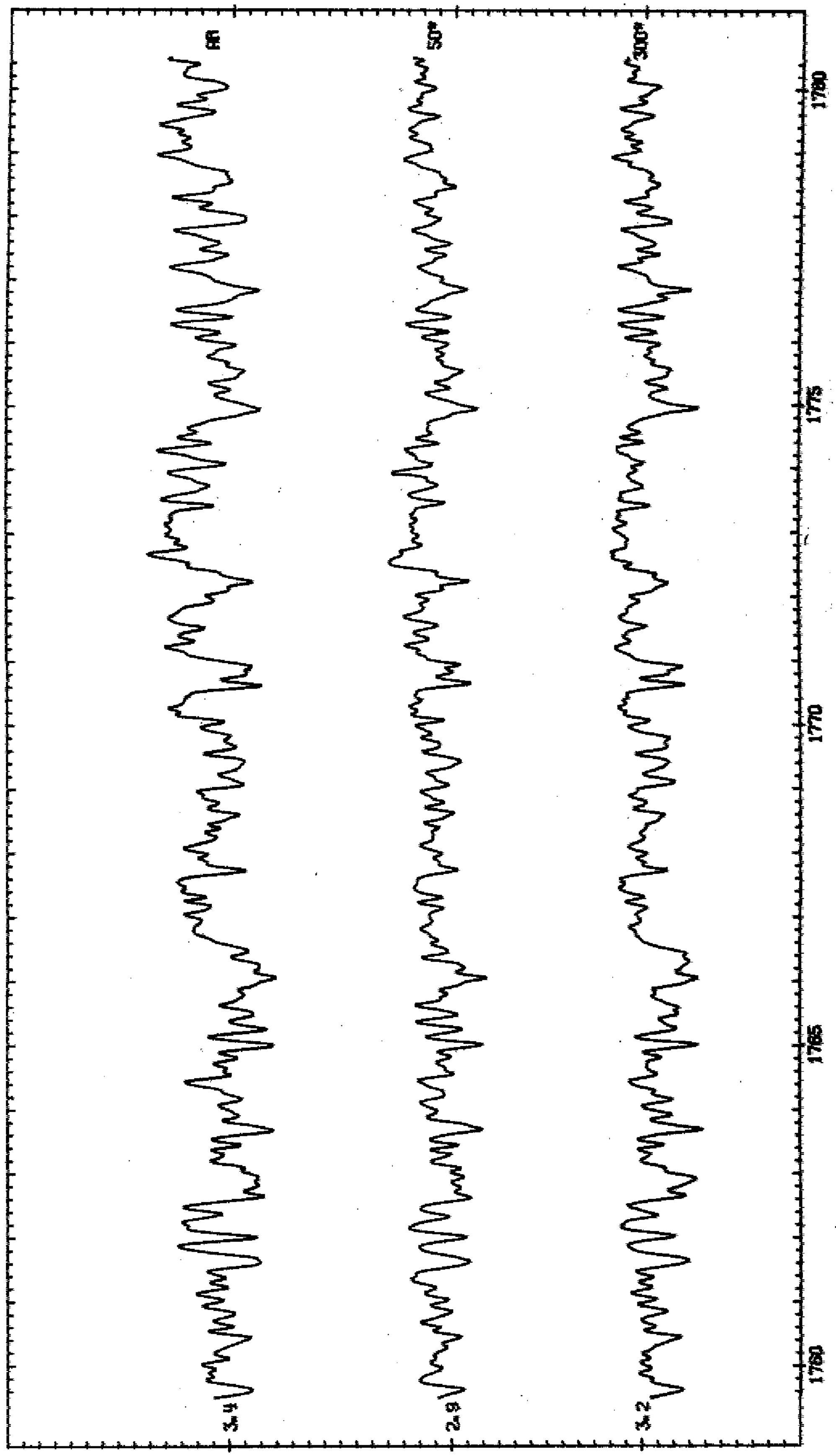
1760
1765
1770
1775
1780
3.4
2.9
3.2
50°
300°

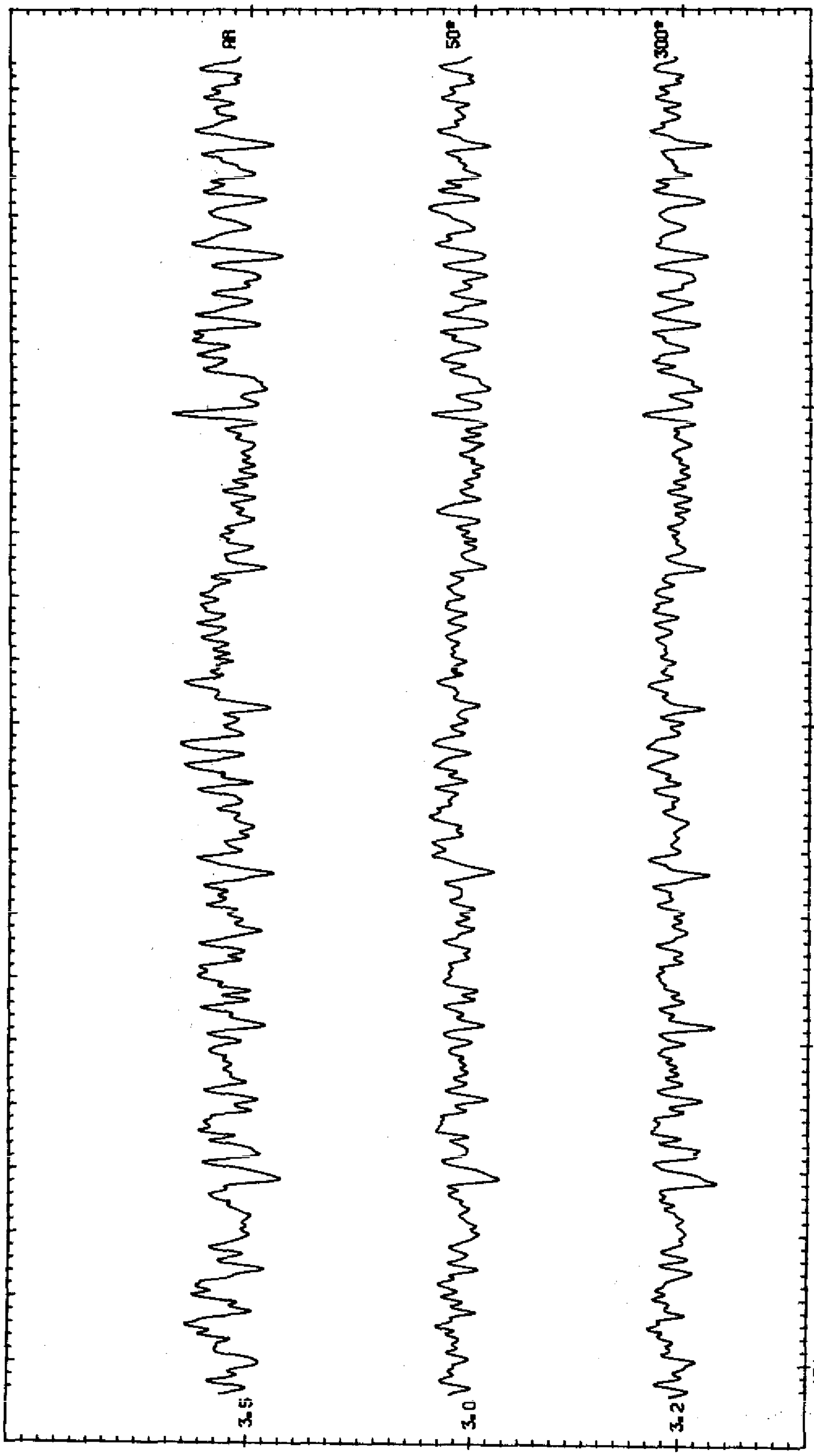
AR
50*
300*
1800
1795
1790
1785
1780
3.5
3.0
3.2

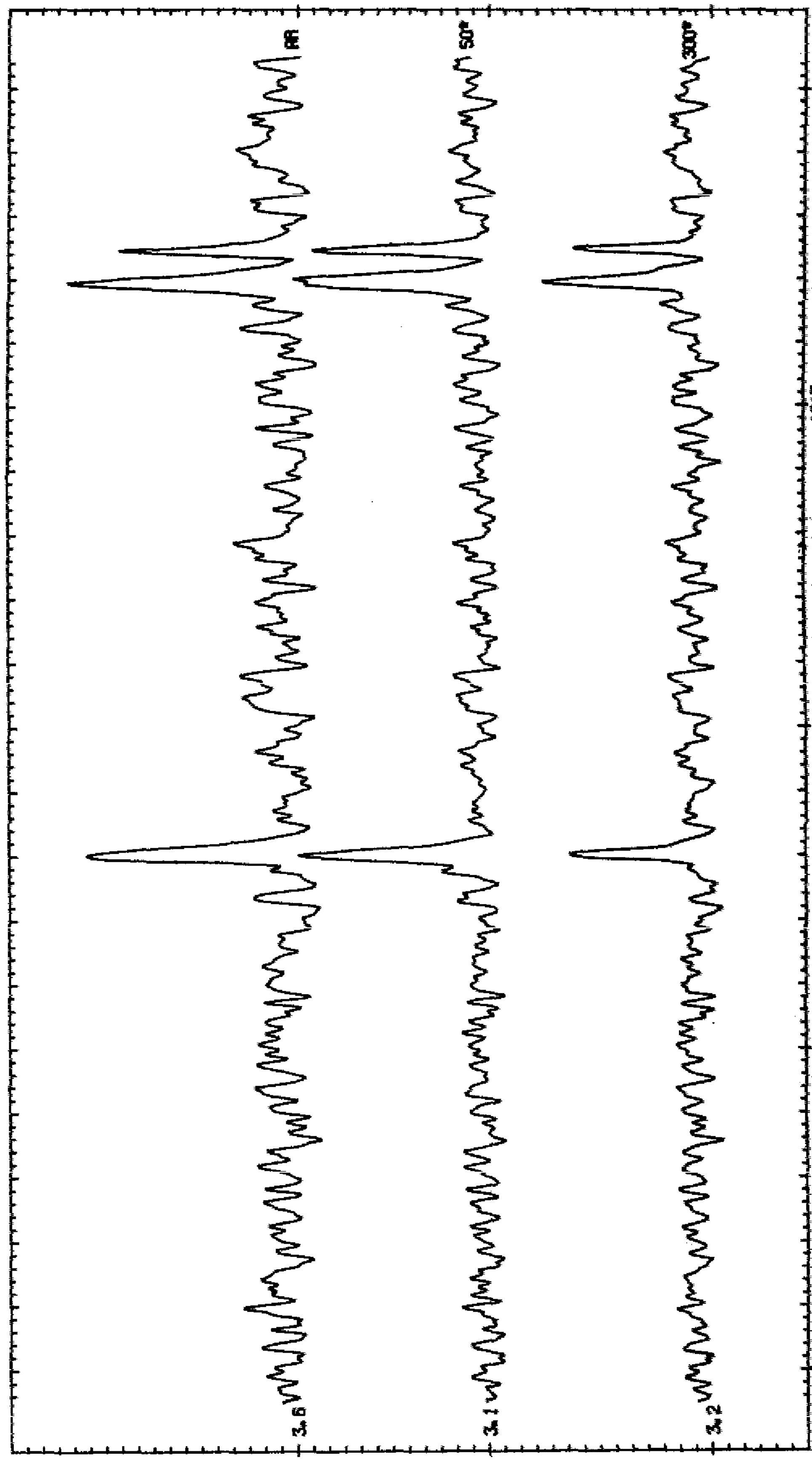
RR
50°
300°
3.6
3.1
3.2
1800
1805
1810
1815
1820

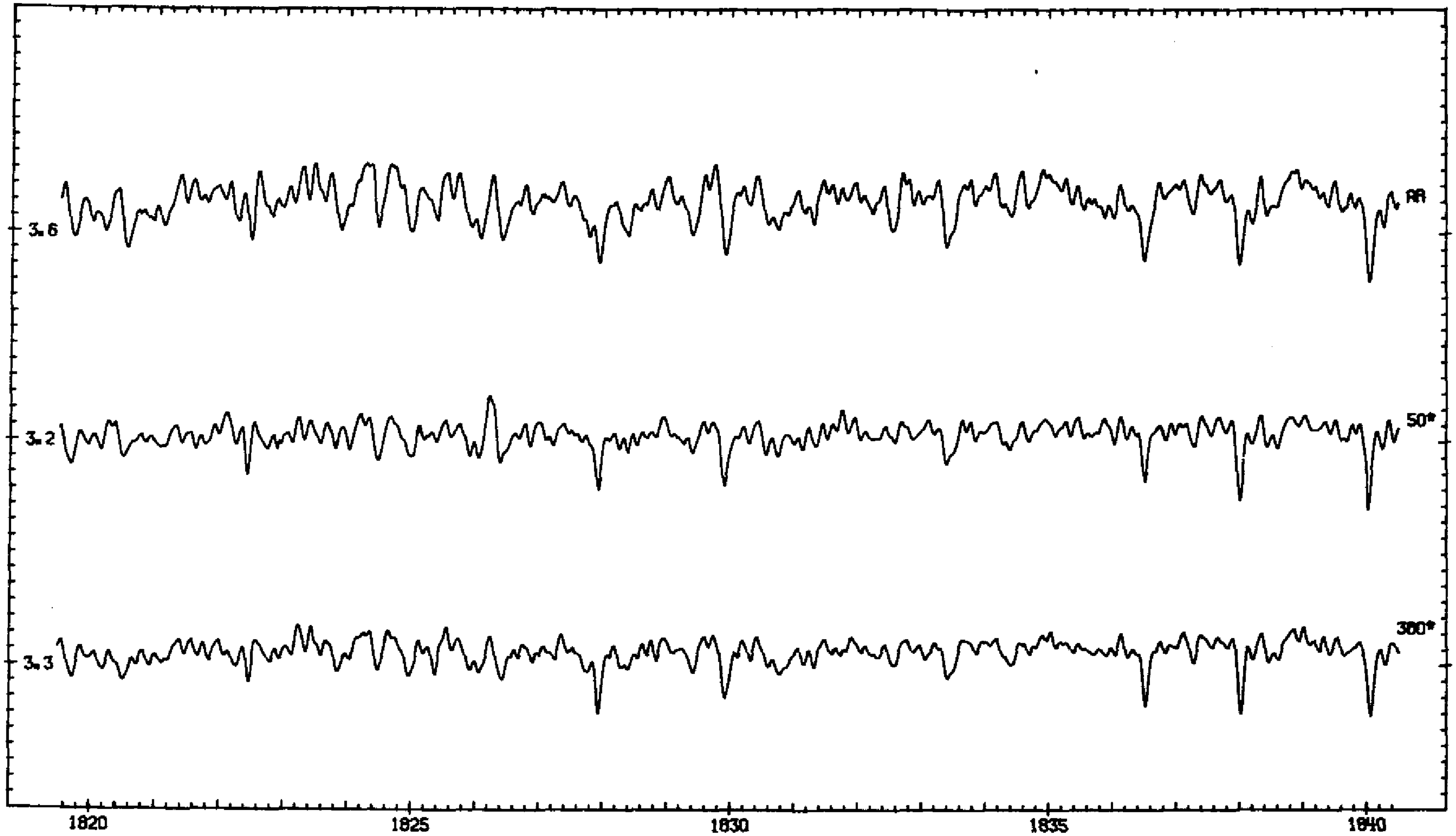

3.6
3.2
3.3
AA
50*
380*
1820
1825
1830
1835
1840

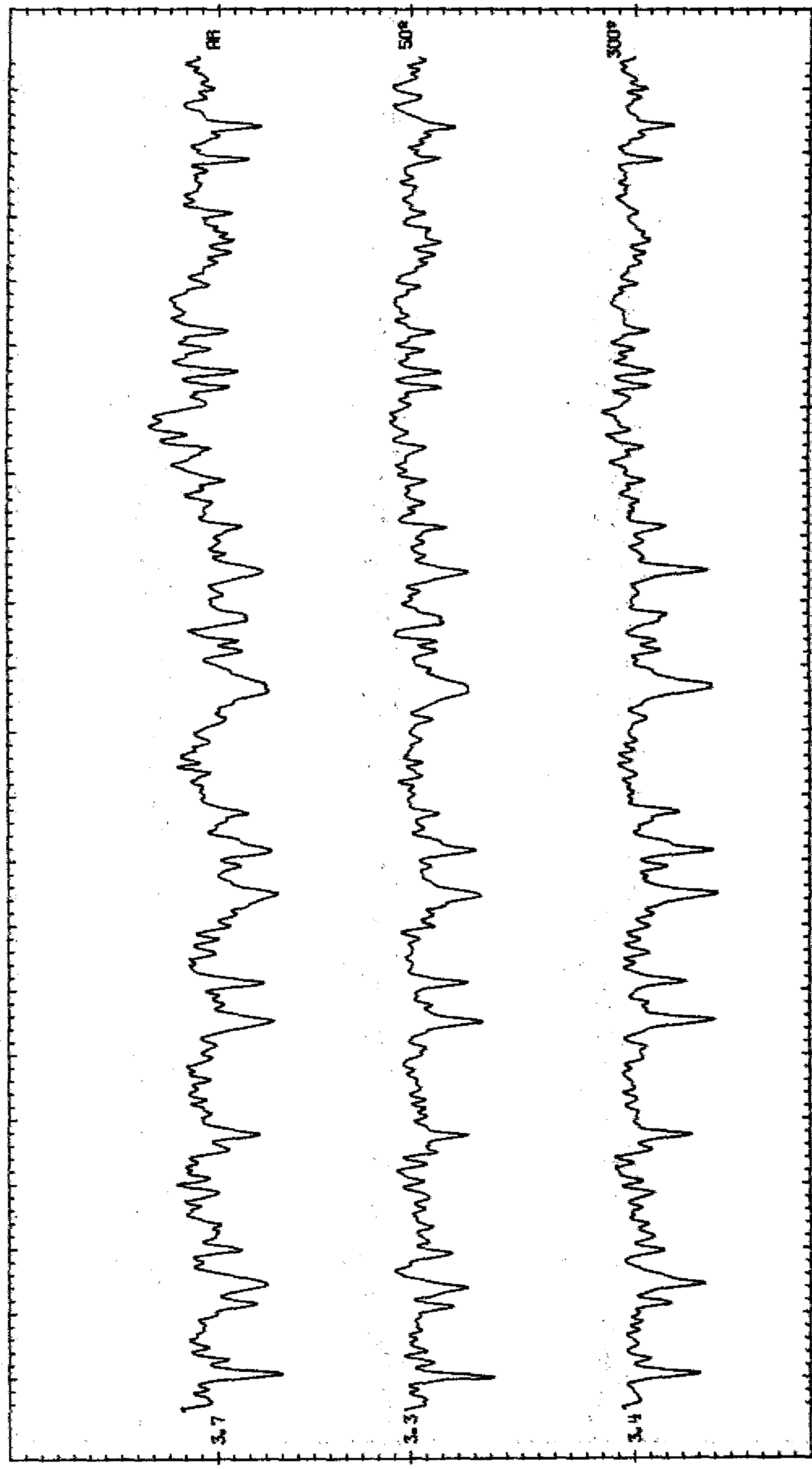
AR
50°
300°
3.7
3.3
3.4
1840
1845
1850
1855
1860

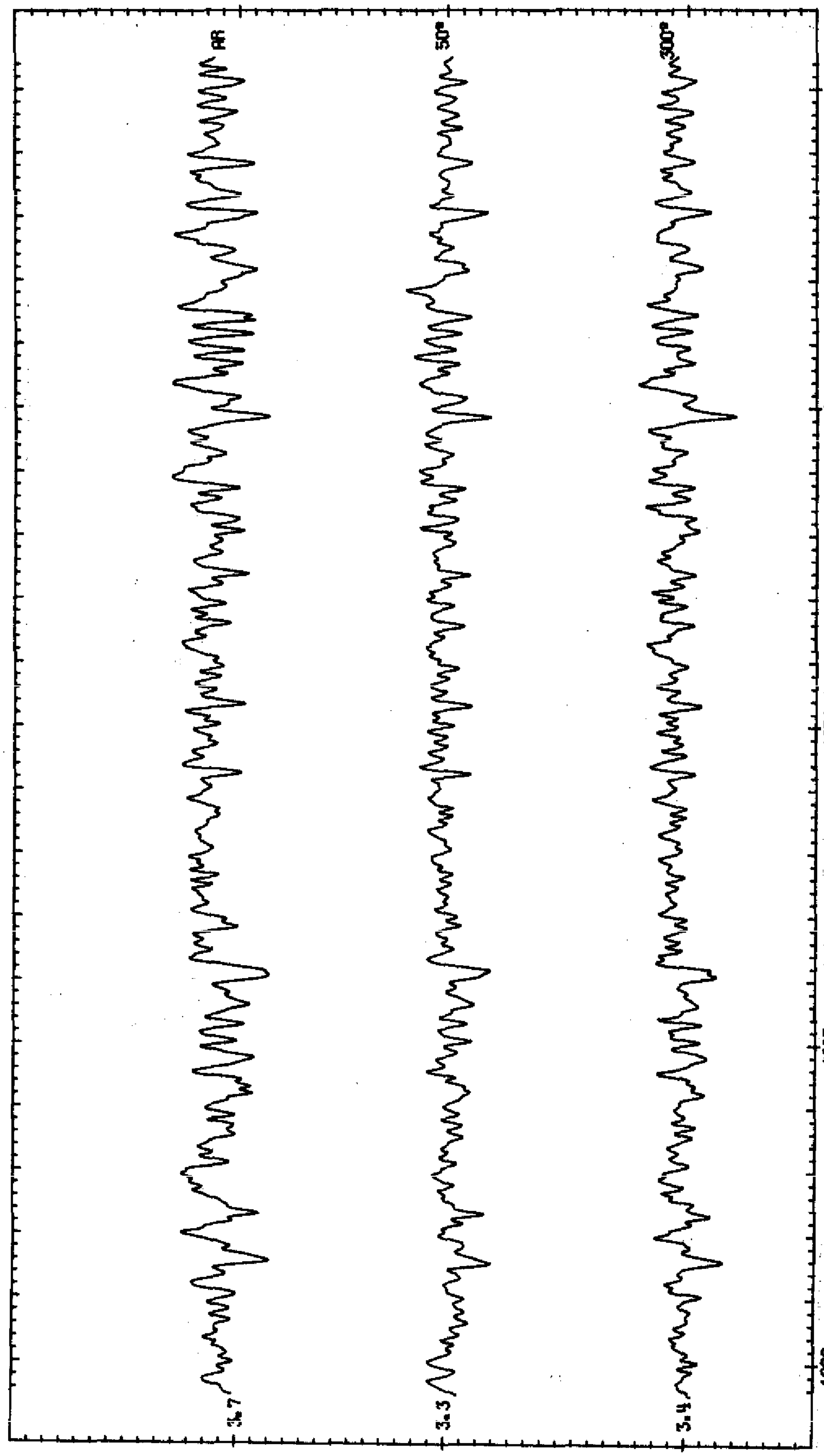
AR
50°
300°
3.7
3.3
3.4
1860
1865
1870
1875
1880

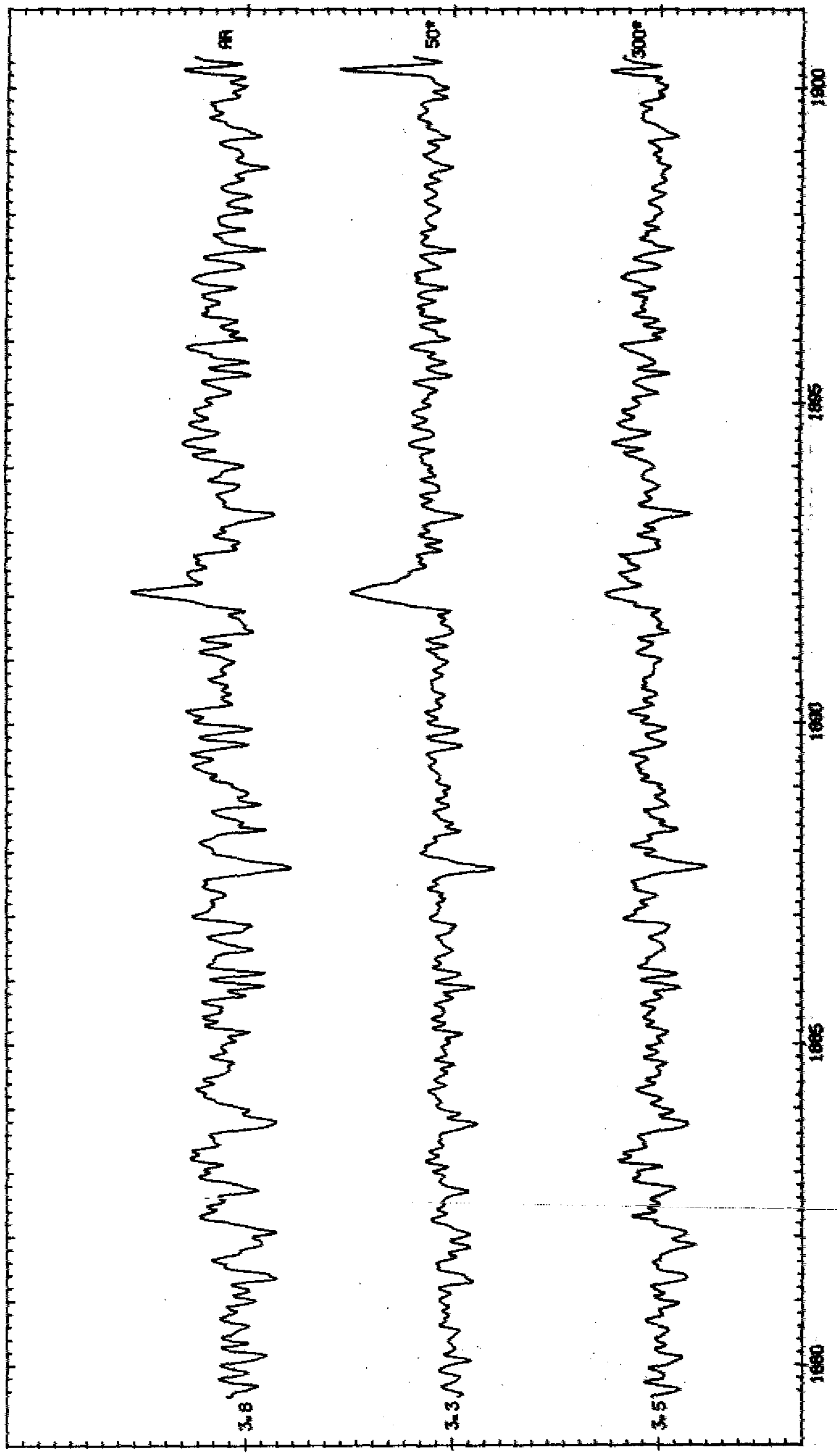
AR
50°
300°
3.8
3.3
3.5
1880
1885
1890
1895
1900

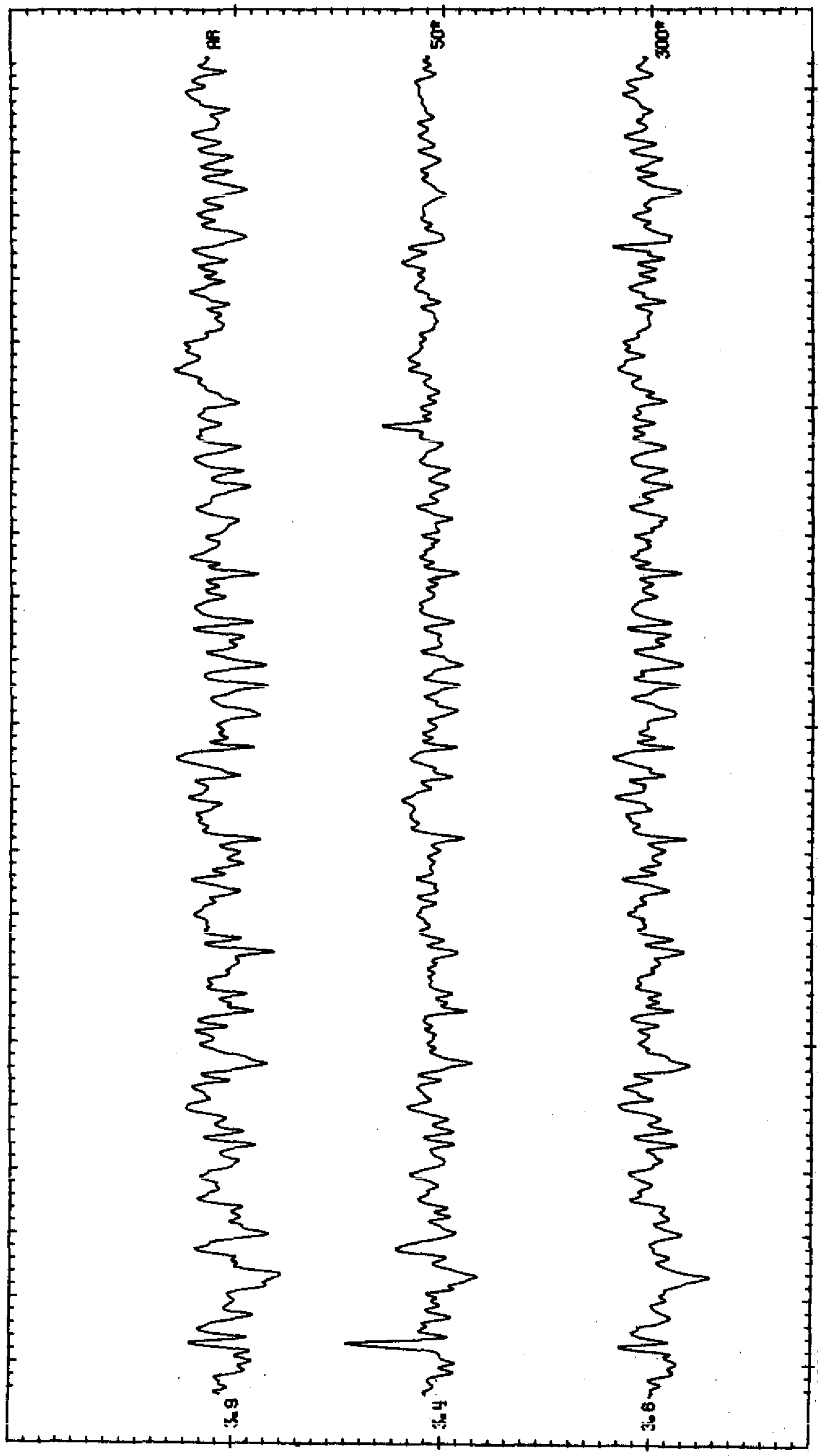
AR
3.9
3.4
3.6
1900
1905
1910
1915
1920

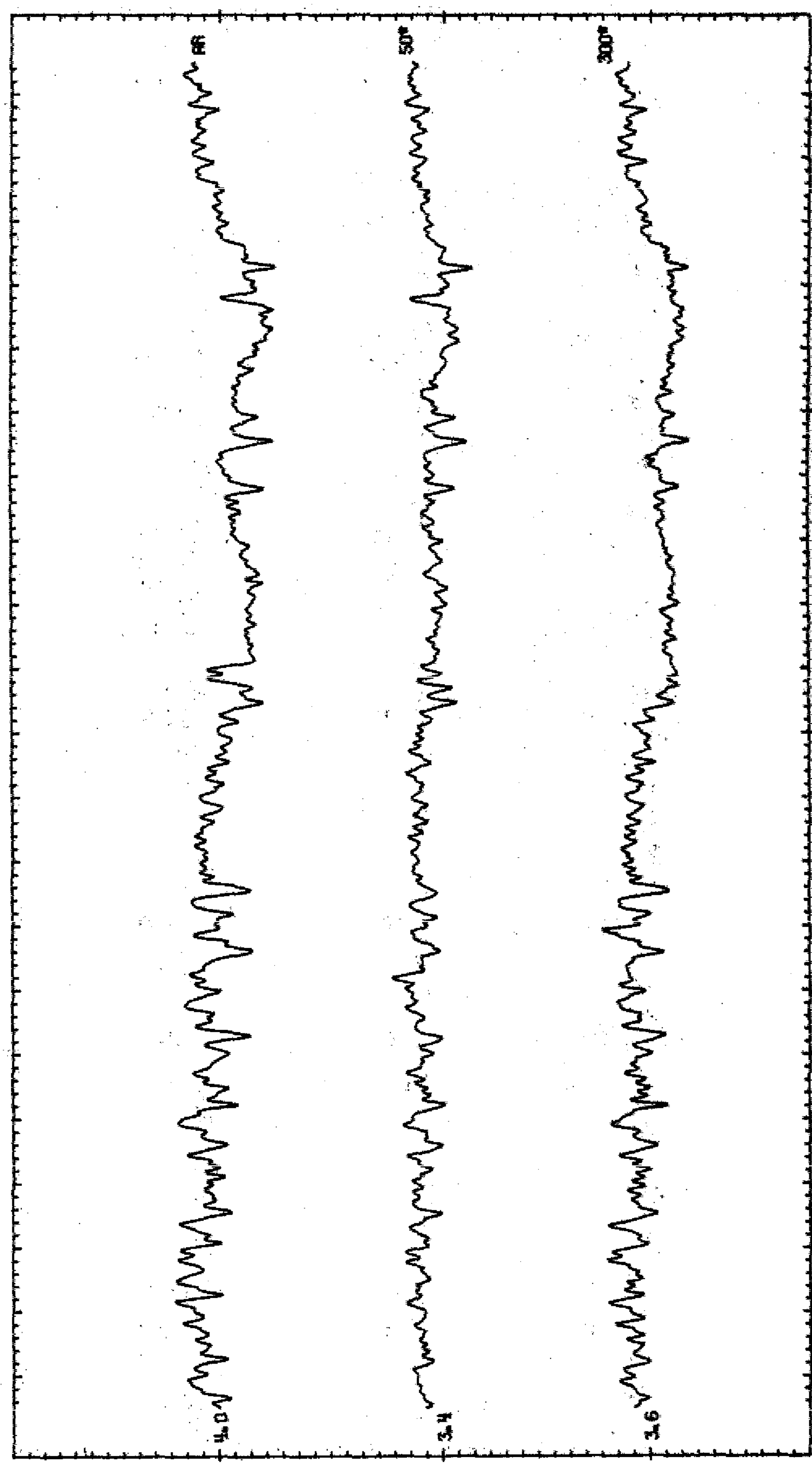
50°
300°
1940
1935
1930
1925
1920
4.0
3.4
3.6

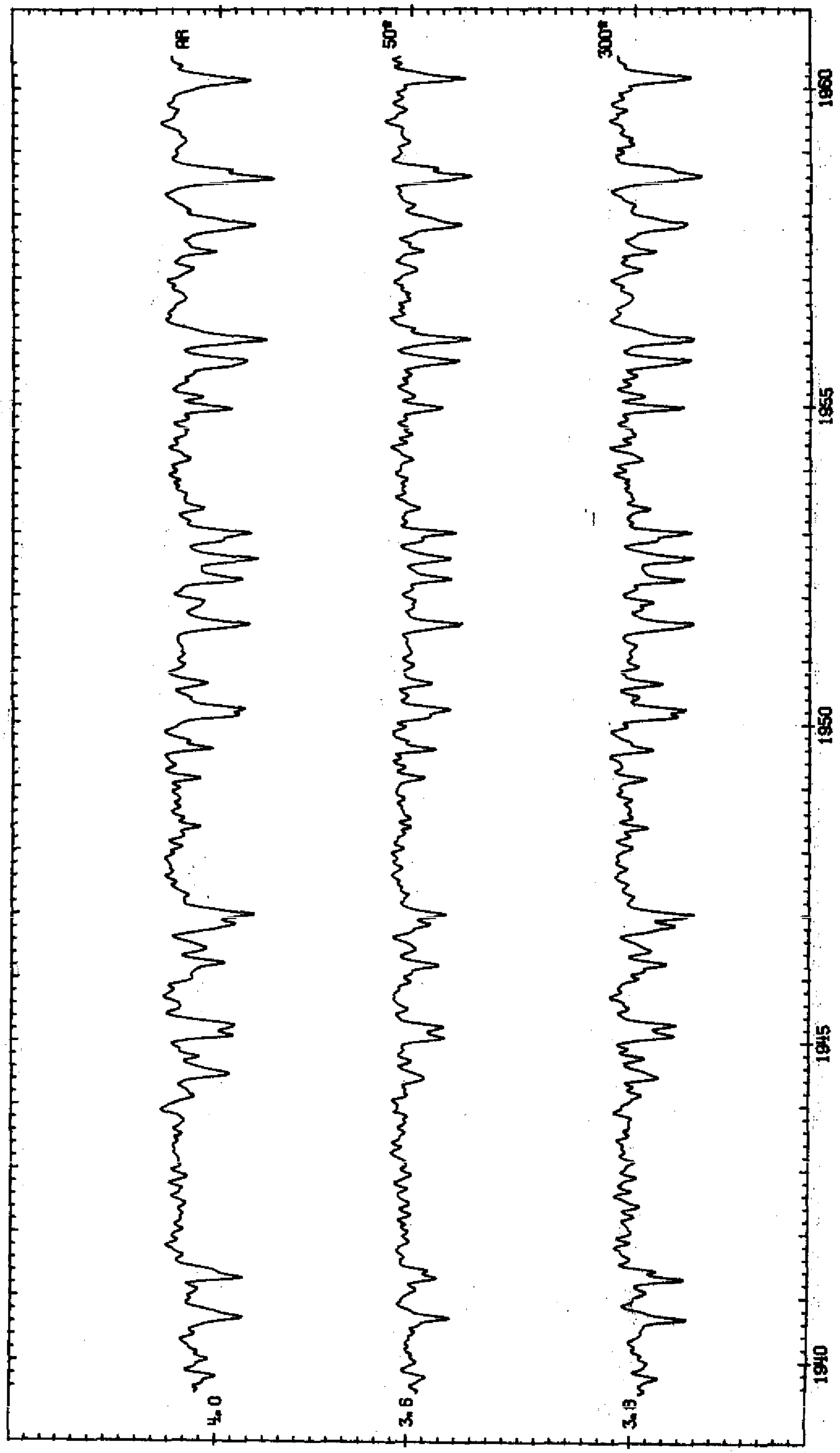
AR
50°
300°
4.0
3.6
1940
1945
1950
1955
1960

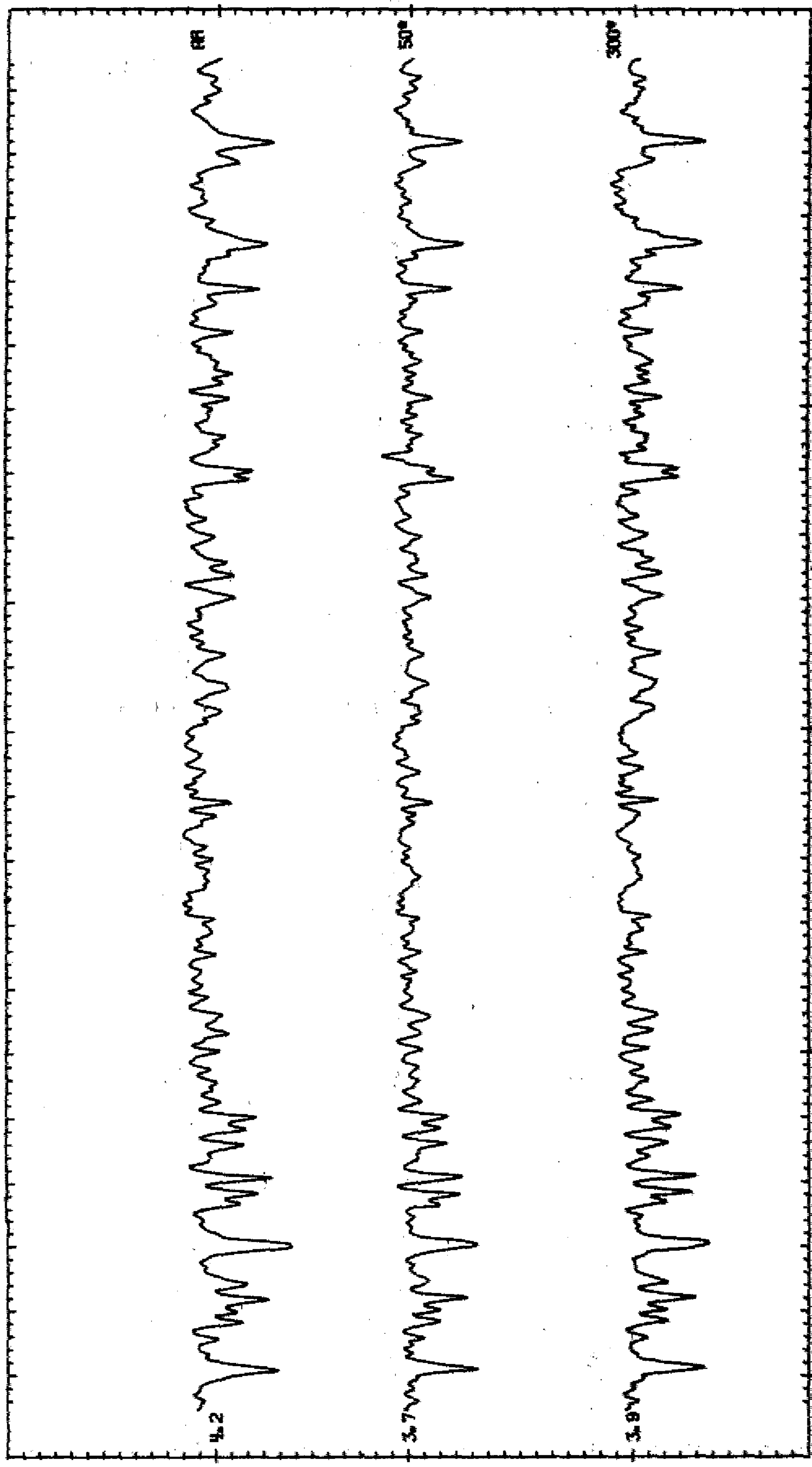

50°
300°
4.2
3.7
3.9
1960
1965
1970
1975
1980

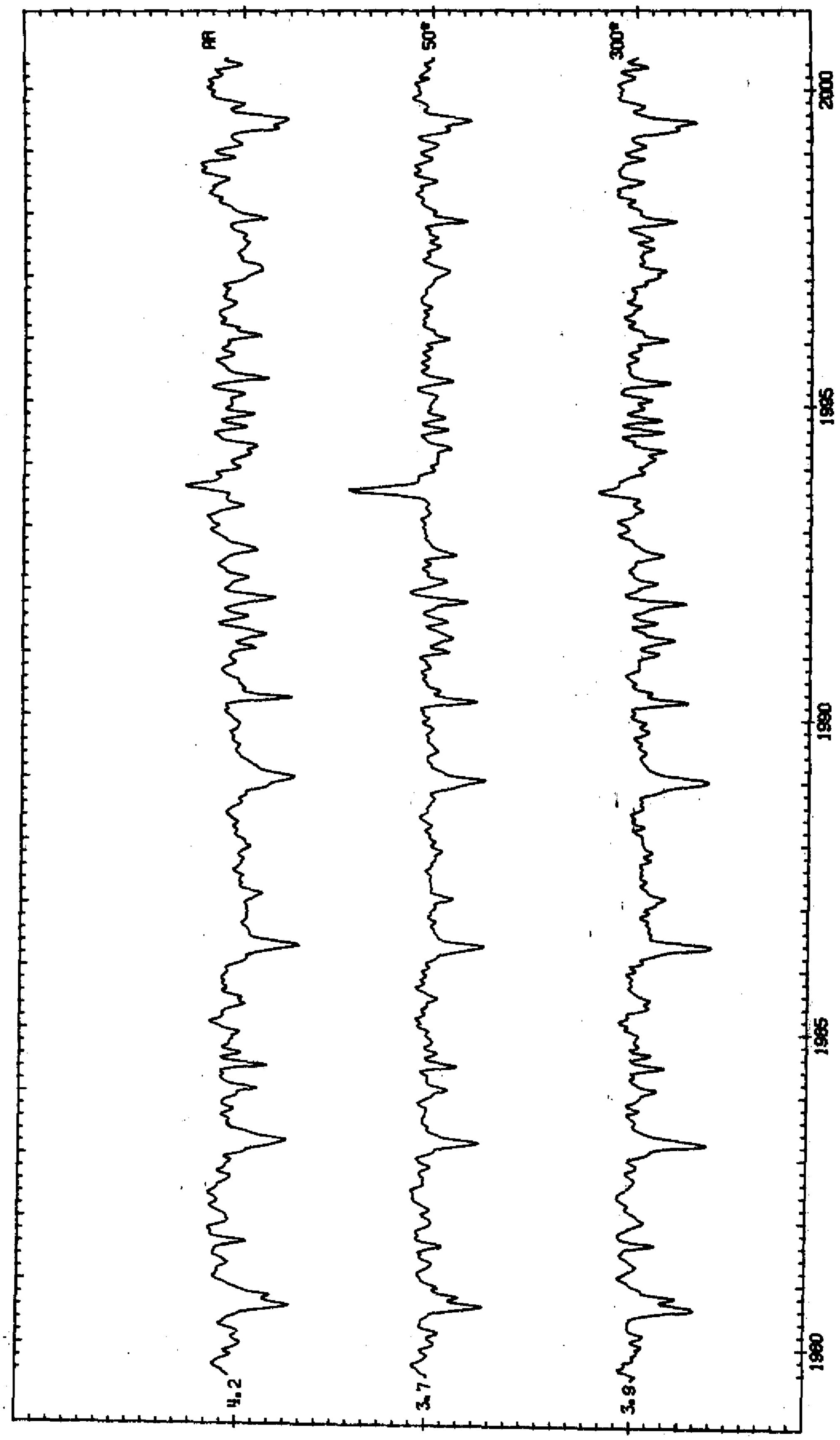

AA
50°
300°
4.2
3.7
3.9
1980
1985
1990
1995
2000

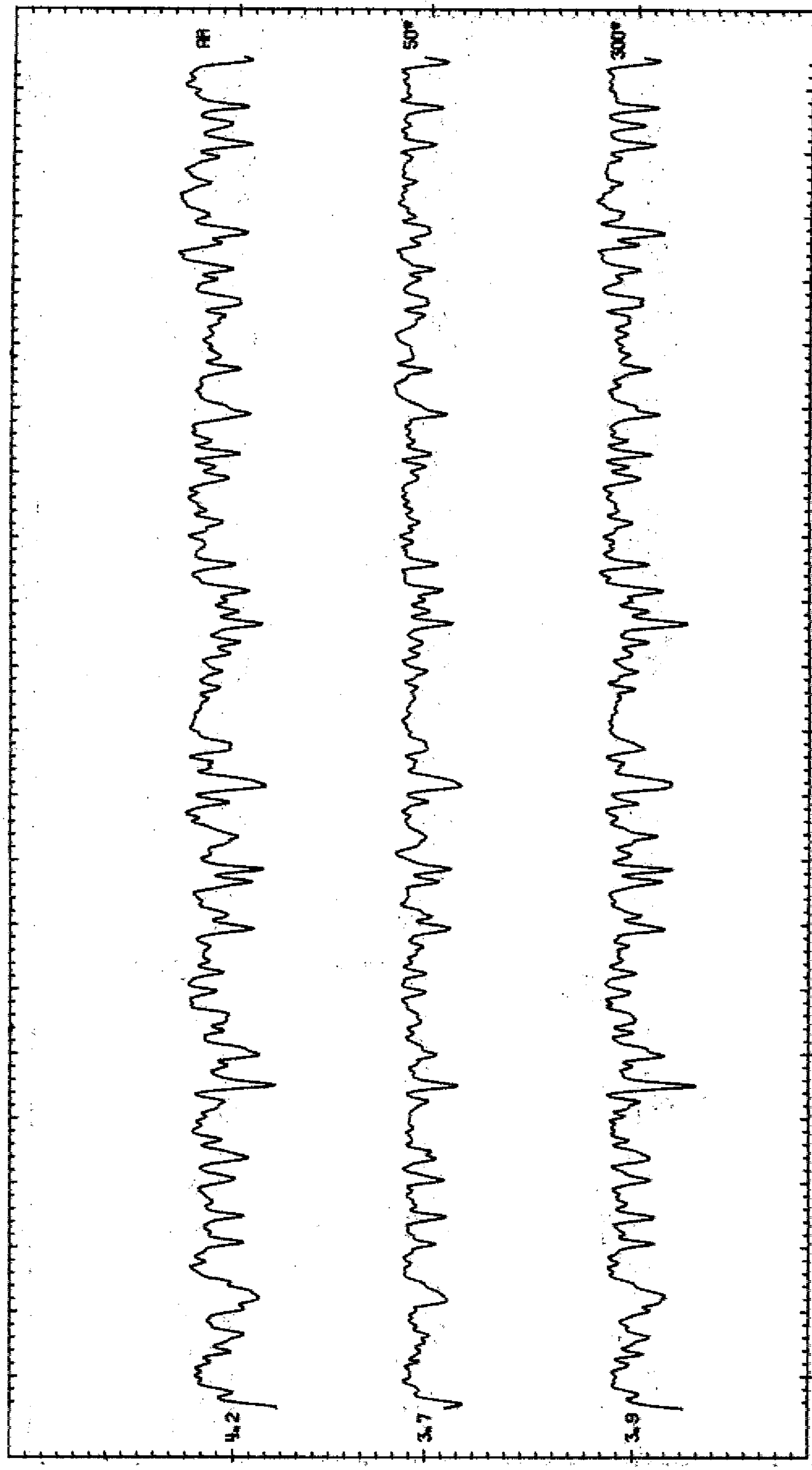
AR
50°
300°
4.2
3.7
3.9
2000
2005
2010
2015
2020

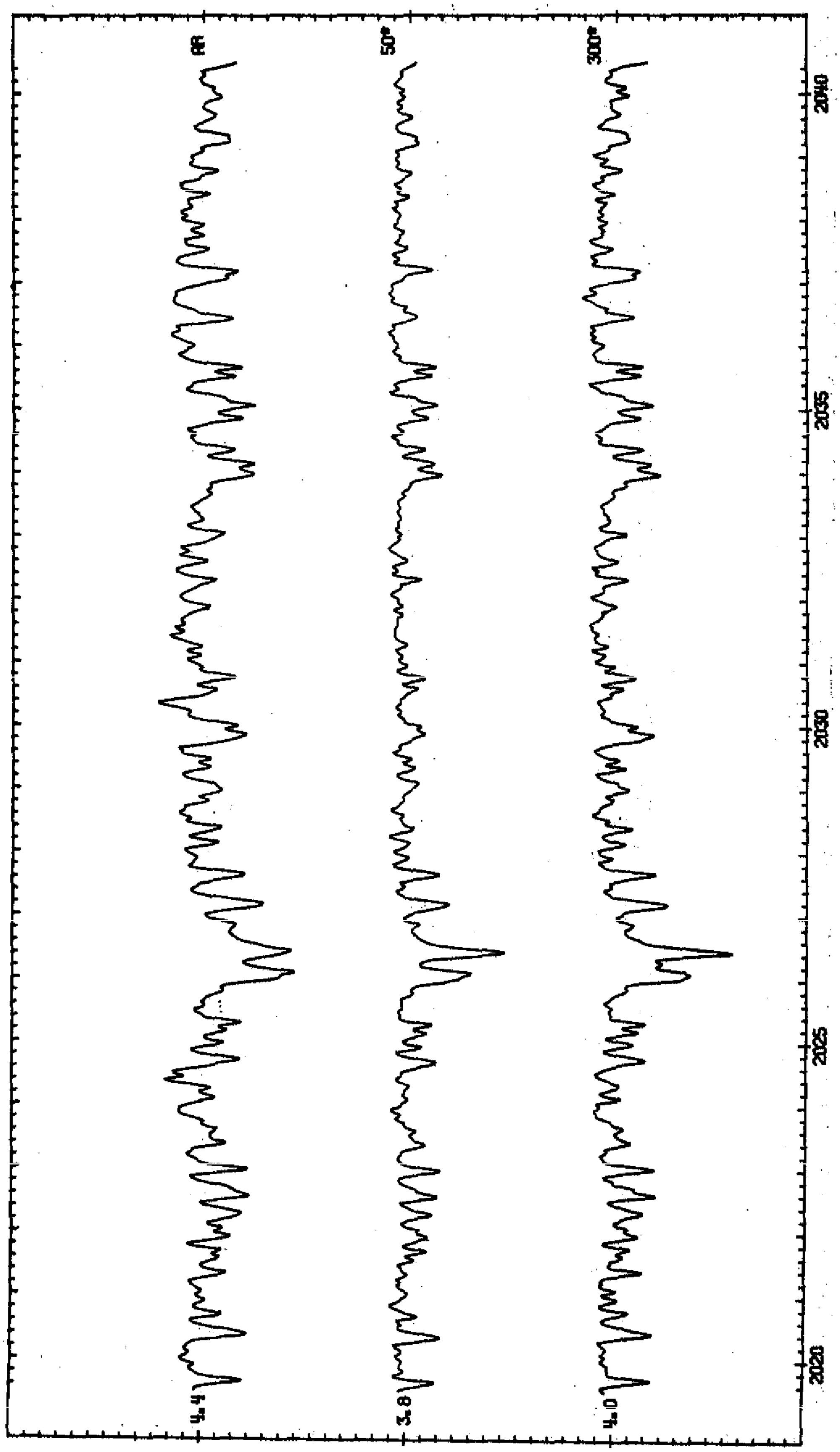
RR
50°
300°
4.4
3.8
4.0
2020
2025
2030
2035
2040

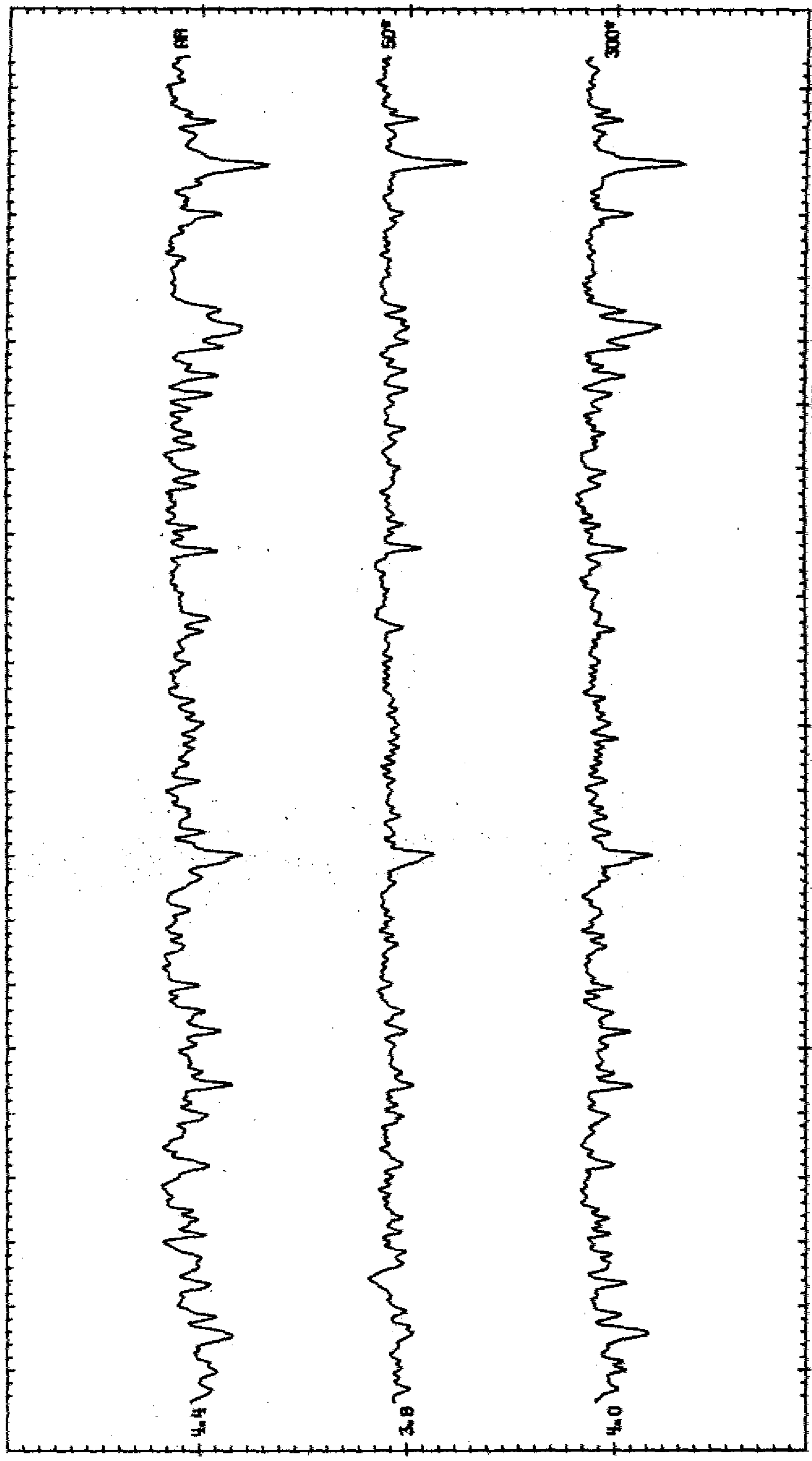
RR
50°
300°
4.4
3.8
4.0
2040
2045
2050
2055
2060

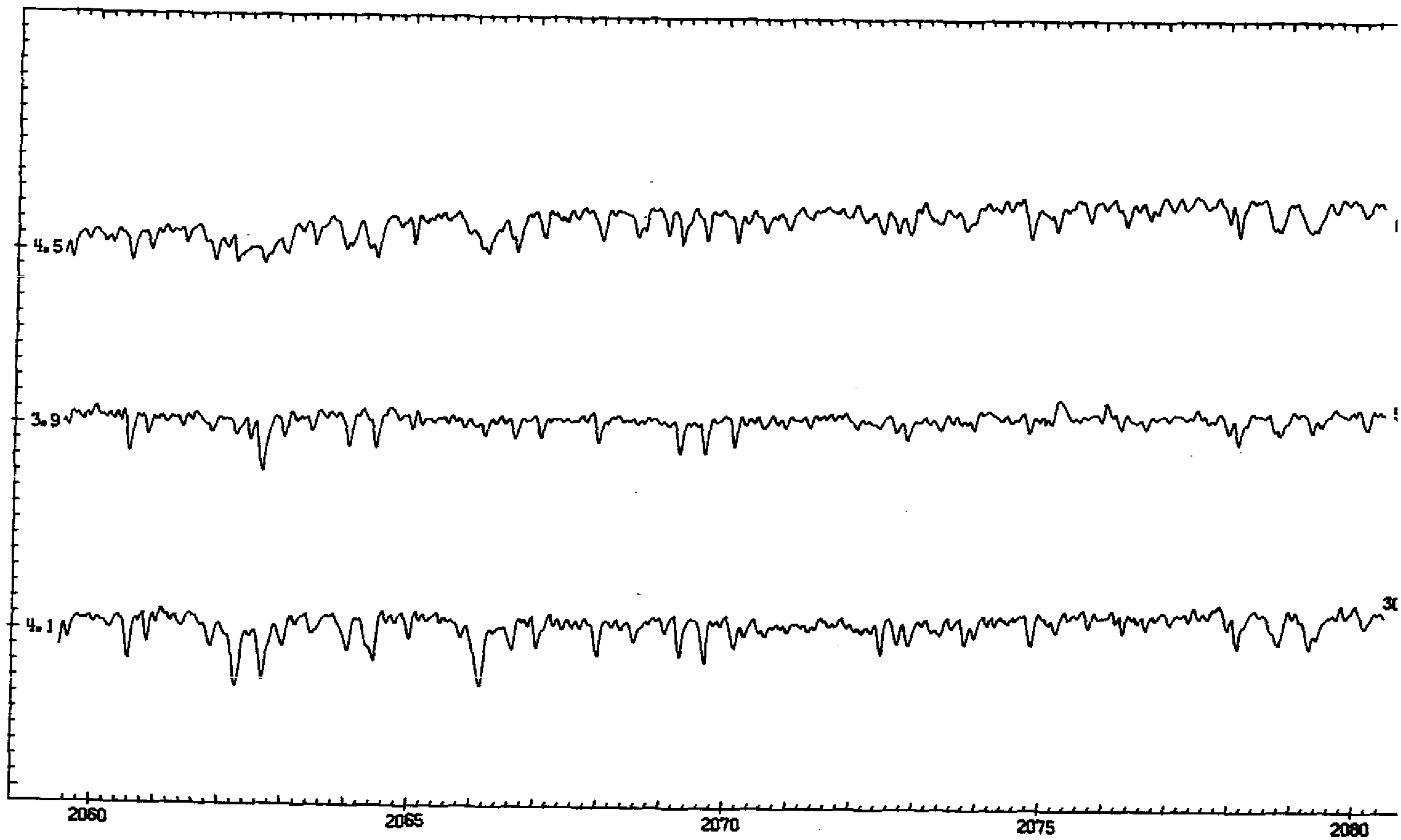
4.5
3.9
4.1
2060
2065
2070
2075
2080

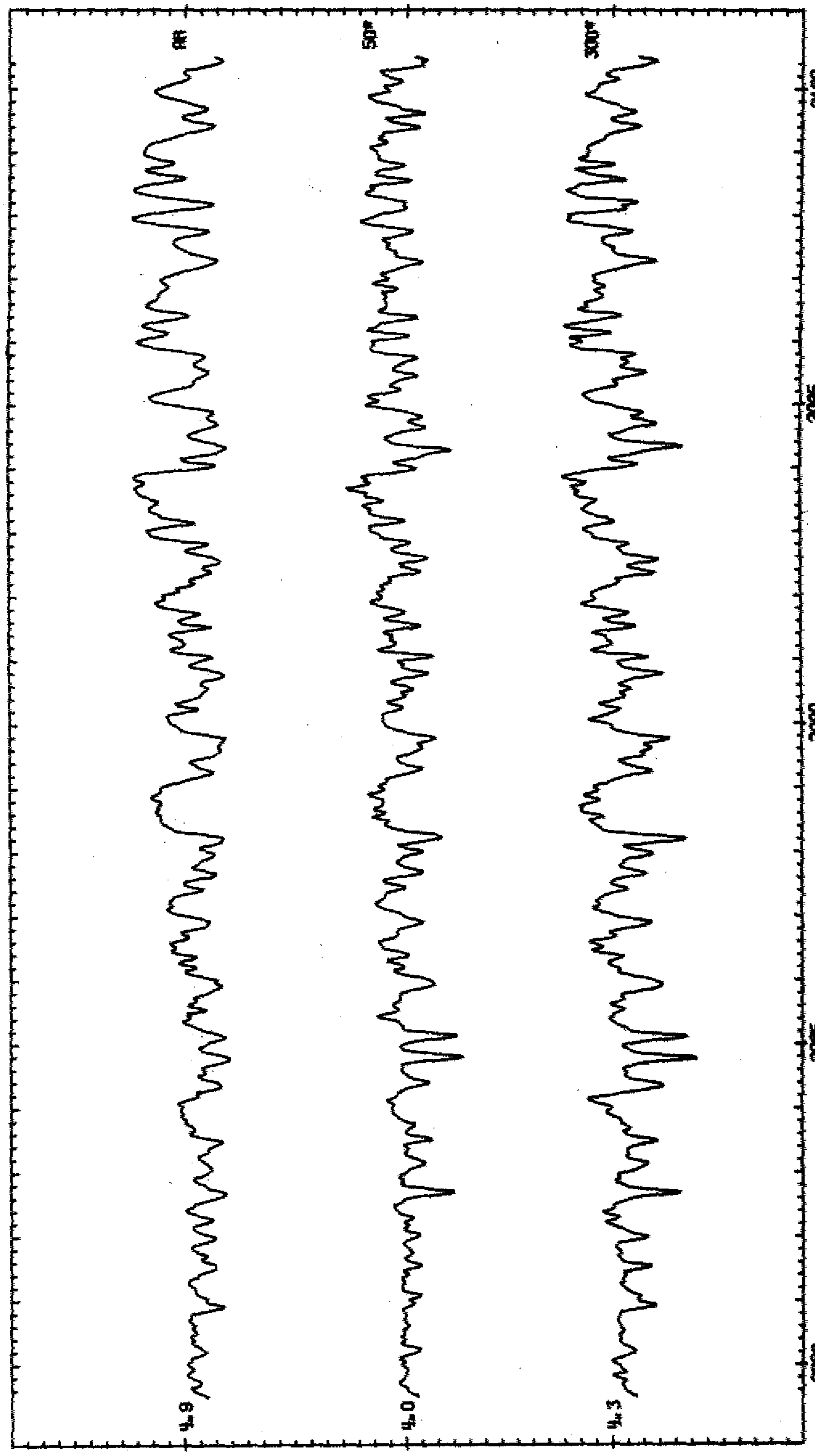

*U.S. GOVERNMENT PRINTING OFFICE: 1977 240-824/001 1-3